



canada/yukon economic  
development agreement

**INDIAN AND NORTHERN AFFAIRS CANADA  
NORTHERN AFFAIRS: YUKON REGION**

**Open File 1996-3(G)**

**GRANITIC PEGMATITES IN  
NORTH-WESTERN CANADA**

by

**LEE A. GROAT  
DEPARTMENT OF GEOLOGICAL SCIENCES  
UNIVERSITY OF BRITISH COLUMBIA**

and

**T. SCOTT ERCIT  
RESEARCH DIVISION  
CANADIAN MUSEUM OF NATURE**

**Canada**

**Yukon**  
Government

14-66

\$50.

**Exploration and Geological Services  
Indian and Northern Affairs Canada  
#345 - 300 Main Street  
Whitehorse, Yukon, Y1A 2B5.**

**INDIAN AND NORTHERN AFFAIRS CANADA  
NORTHERN AFFAIRS: YUKON REGION**

**Open File 1996-3(G)**

**GRANITIC PEGMATITES IN  
NORTH-WESTERN CANADA**

**by**

**LEE A. GROAT  
DEPARTMENT OF GEOLOGICAL SCIENCES  
UNIVERSITY OF BRITISH COLUMBIA  
VANCOUVER, B.C., V6T 1Z4**

**and**

**T. SCOTT ERCIT  
RESEARCH DIVISION  
CANADIAN MUSEUM OF NATURE  
OTTAWA, ONTARIO, K1P 6P4**

**August 1996**

## TABLE OF CONTENTS

1. INTRODUCTION	4
1.1 Granite-Pegmatite Systems	5
1.2 Fertile Granites in the Canadian Cordillera	5
2. LITERATURE SEARCH	6
3. ANALYTICAL METHODS	7
4. PREVIOUS WORK AND THE 1995 FIELD SEASON	7
5. HORSERANCH RANGE	7
6. MCQUESTEN RIVER REGION	8
7. ICE LAKES AREA, CASSIAR BATHOLITH	9
8. CASSIAR BATHOLITH, EASTERN MARGIN	10
9. CLEA PLUTON, SELWYN PLUTONIC SUITE	11
10. THE LITTLE NAHANNI PEGMATITE GROUP	12
10.1 Geological Setting	12
10.2 Description of the Pegmatites	12
10.3 Geochronology	15
11. THE O'GRADY BATHOLITH	15
11.1 Mineral Chemistry	17
11.2 Whole-Rock Geochemistry	20
11.3 Origin of the Li-Enriched Pegmatites	20
12. PROSPECTING FOR RARE-ELEMENT BEARING PEGMATITES	21
13. SCIENTIFIC COMMUNICATIONS	22
13.1 Refereed Journal Publications	22
13.2 Refereed Conference Abstracts	22
14. BENEFIT TO THE YUKON TERRITORY	23
15. SUGGESTIONS FOR FUTURE WORK	24
15.1 Seagull Batholith	24
15.2 Thirtymile Pluton and Ork Stock	25
15.3 Mount Mye Batholith, Anvil Plutonic Suite	25
15.4 Lened, CAC, and RUDI Plutons	25
15.5 Sekwi Mountain Map Area	25

15.6 Macmillan Pass	26
15.7 Mid-Cretaceous Suite, Intermontane Belt	26
15.8 Emerald Lake	26
16. ACKNOWLEDGEMENTS	26
17. REFERENCES	28
LIST OF FIGURES	31
APPENDIX 1	
APPENDIX 2	

## 1. INTRODUCTION

This report is one of a series (Groat *et al.* 1994, 1995a, 1995b, 1996) on the results of our research on granitic pegmatites in northwestern Canada. These unusual rocks are of scientific and economic interest for the following reasons:

1. Rare elements such as tantalum, niobium, lithium, rubidium, cesium, beryllium, and tin are commonly found in granitic pegmatites, and can occur in concentrations sufficiently high to warrant mining operations (*e.g.*, Bernic Lake, Manitoba). Ta and Nb are used in prostheses, capacitors, laser crystals, and piezoelectric instruments; Li is medicinally important for the treatment of manic depression, is used in advanced technology batteries, and is a key ingredient of specialized glassware (see front-page article in the *Globe and Mail*, September 26, 1994); and Be and Sn are industrially important as components of alloys.
2. Granitic pegmatites host a diversity of rare mineral species, and are a globally important source of gemstones such as emerald, topaz, aquamarine and tourmaline. Pegmatites in western North America have known gemstone potential.
3. Granitic pegmatites reveal information about melting of rocks in the lower crust and are an important source of information regarding fractionation of felsic magma suites, especially extreme fractionation. The minerals from granitic pegmatites were among the first to be used in absolute (radiometric) dating; granitic pegmatites are of importance in relative and absolute dating of the late stages of tectonic events.

This research project involves the study of granitic pegmatites from the Canadian Cordillera in northern British Columbia and the Yukon and Northwest Territories. Considerable research has been done on granitic pegmatite suites from the Canadian Shield; by comparison, the pegmatite potential of the Cordilleran region is largely unknown. Our study represents the first attempt ever to conduct original research on the regional geology of Cordilleran pegmatites.

## 1.1 Granite-Pegmatite Systems

Pegmatites represent end-products of the magmatic stage in the evolution of granitic melts. The appreciable degrees of fractionation required to produce granitic pegmatites can result in significant accumulations of large-ion lithophile elements (LILE) such as Li, Rb, and Cs, and high field-strength elements (HFSE) such as Nb, Ta, and Sn. As such, granitic pegmatites sometimes host economic concentrations of the rare metals Li, Rb, Cs, Ta, Nb, Sn and Be (e.g., Tanco pegmatite, Manitoba).

Granitoids parental to rare-element-enriched pegmatites ("fertile") have features which distinguish them from other ("barren") granitoids: these features serve both as a prospecting tool for selecting regions worthy of study, and are prophetic of the degree of rare-element enrichment of associated pegmatites. Fertile granites are typically late- to post-tectonic and emplaced at moderate to shallow crustal levels. They are typically texturally inhomogeneous, often with megacrystic ("pegmatoid") pods or regions. They are highly silicic, leucocratic and meta- to peraluminous, often expressed in the accessory mineralogy (cordierite, andalusite or garnet-bearing). They are typically mica-bearing; best prospects are two-mica granites, but biotite granites and, rarely, biotite-hornblende granites have been known to generate rare-element-enriched pegmatites. They generally carry a S-type geochemical signature (White & Chappell 1983); initial  $^{87}\text{Sr}/^{86}\text{Sr}$  isotopic ratios are high, and K/Rb, K/Cs and K/Li ratios are low.

## 1.2 Fertile Granites in the Canadian Cordillera

Granitoid rocks are widely distributed in the Canadian Cordillera; however, Sr isotope geochemistry indicates a strong tectonic control over the distribution of evolved granites in the Cordillera. Granitoids with Sr isotopic signatures and trace-element chemistry typical of S-type plutonism (Anderson 1988) are localized in the Omineca and Foreland Belts. Largely the products of partial melting of older Precambrian and Paleozoic supracrustal rocks during regional compression and thickening, they denote a mid-Cretaceous plutonic event represented in the northern Cordillera by the Selwyn and Cassiar plutonic suites, and in the southern Cordillera by the Bayonne suite. Plutons of the northern suite are occasionally associated with Sn-tungsten skarn mineralization. For some of these occurrences, aplite and pegmatite dykes are most abundant in

high-grade ore zones (*e.g.*, Mactung; Atkinson & Baker 1983); despite extensive work upon skarn mineralization, little has been done to assess the rare element potential of associated pegmatites.

## 2. LITERATURE SEARCH

The study began with a comprehensive literature search to identify pegmatites of interest. We also used the following characteristics to identify possible fertile granites:

1. Parent granites are usually isolated, small stocks, typically < 30 km<sup>2</sup> in size; however, they are sometimes found as apophyses and at the margins of larger intrusions (batholiths).
2. They are S-type granites, meaning that they are derived from supracrustal (often sedimentary) source material (White & Chappell 1983).
3. For the Cordillera, fertile granites rich in rare elements are usually mid-Cretaceous in age (Armstrong 1988).
4. They are peraluminous (ASI index 1-2), often megacrystic and leucocratic.
5. They show initial <sup>87</sup>Sr/<sup>86</sup>Sr ratios greater than 0.7100 (often 0.7200 to 0.7400) and they have large negative εNd values (typically -6 to -9).
6. They often have a peraluminous accessory mineralogy (two-mica granites, garnet- or andalusite-bearing) or rare-element bearing accessory mineralization (lepidolite = Li).
7. Their whole-rock geochemistry is rich in LILE and HFSE.

Using these criteria, we identified a number of areas of interest in northern British Columbia and the Yukon and Northwest Territories.



### 3. ANALYTICAL METHODS

Electron microprobe analyses were done at the Canadian Museum of Nature, using a JEOL 733 microprobe with Tracor-Northern 5500 and 5600 automation. Operating conditions were (in general) 15 kV and 20 nA, with a maximum count time of 25 s. Data were reduced with a conventional ZAF routine. Undetected constituents ( $\text{Li}_2\text{O}$ ,  $\text{B}_2\text{O}_3$ ,  $\text{BeO}$ , and  $\text{H}_2\text{O}$ ) were calculated according to mineral stoichiometry.

Whole-rock analyses were done by Chemex Labs Limited of North Vancouver.

### 4. PREVIOUS WORK AND THE 1995 FIELD SEASON

The study began with a comprehensive literature search in 1991. The next summer we spent one week studying the Little Nahanni Pegmatite Group, and one week in the Horseranch Range in northern British Columbia. The following year (1993) we worked for over a month in the LNPG area. In 1994 we spent a total of six weeks in the Northwest and Yukon Territories, studying the LNPG, O'Grady batholith, Clea pluton, and the northwest margin of the Cassiar batholith in the Ice Lakes area. In 1995 we spent more than a month visiting the LNPG, the O'Grady batholith, the Horseranch Range, and the eastern side of the Cassiar batholith. Field work in 1994 was hampered by extensive forest fires, and in 1995 by very poor weather.

The individual pegmatite localities are described in the following sections, beginning with northern British Columbia, followed by the Yukon Territory (from west to east), and the Northwest Territories. The last two localities (LNPG and O'Grady) are described in more detail because the pegmatites found there are the most highly fractionated, and are therefore of greatest geochemical interest. They also help to illustrate the degree of fractionation present in the more primitive pegmatites found in northern British Columbia and the Yukon Territory.

### 5. HORSERANCH RANGE (BC; 59°21'N, 128°52'W)

This locality includes the 26 Cassiar Beryl claims, staked in 1955 to cover occurrences of beryl in pegmatite in the central part of the Horseranch Range (see Mulligan 1968). We spent several

weeks in the area in both 1992 and 1995. The pegmatites occur on the western side of the range, and are especially common around the cirque drained by Camp Creek (local name). They intrude foliated metasedimentary rocks of the Horseranch group, and range in width from a few cm to several m. In general, the pegmatites are parallel to the foliation (approximately NW).

Mineralogically, the pegmatites are composed of feldspar, quartz, muscovite, black tourmaline, and minor amounts of pale-green beryl and garnet. The beryl generally occurs as hexagonal prisms from a few mm in width to several cm across. Some zoning is seen in the narrower dikes.

What we assume to be a granite parental to the pegmatites was discovered on the south side of Camp Creek. Whole rock and mineral analyses are needed to confirm the relationship between the pegmatites and the granite. Very little analytical work has been done to date because we have concentrated on pegmatites in the Yukon and Northwest Territories. However, preliminary electron microprobe analyses of garnets (Fig. 2), tourmalines (Fig. 3), feldspars and micas (Fig. 4) from the Horseranch pegmatites suggest an intermediate degree of fractionation. The analyses also suggest that beryl from more primitive pegmatites (such as Horseranch and Ice Lakes) have higher Fe and lower alkali and H<sub>2</sub>O contents than beryl from more highly fractionated pegmatites (such as LNPG).

## 6. McQUESTEN RIVER REGION (YT; 63°47'N, 137°25'W)

Two-mica granites in the McQuesten River region of central Yukon are similar to those in the Selwyn Suite, thus are potentially parental to rare-element pegmatites. LAG and TSE spent several days in late July, 1994, studying granitoid plutons in the area, in the company of D. Murphy and J. Mortensen. Subsequent to this, we examined an additional pluton in the area (the Two Sisters batholith) in detail. The Two Sisters batholith is a late Cretaceous (65 Ma), medium to coarse grained, locally porphyritic two-mica granite. We examined the northern margin of the batholith, where a megacrystic marginal phase is exposed. Numerous small, black tourmaline-bearing, coarse-grained segregations are present in the marginal phase, but pegmatites *sensu stricto* are conspicuously absent. The presence of tourmaline in the segregations indicates local enrichment in boron, which is a potential indicator of rare-metal enrichment. However, there are no mineralogical indicators of rare-metal mineralization (*i.e.*, no rare-metal oxides of Sn, Ta or Nb,

nor coloured tourmaline indicative of Li enrichment). Whole rock and mineral analyses are needed to confirm these observations.

#### 7. ICE LAKES AREA, CASSIAR BATHOLITH (YT; 60°22.5'N, 131°20'W)

The Cassiar batholith is known for associated tin skarns, but very little is known of the beryllium potential of the batholith. Mulligan (1968) was the first to note the association of beryllium mineralization with the Cassiar batholith, in the form of an occurrence of beryl within a single pegmatite dike. Consequently, previous to our studies, nothing was known of the extent or relative concentration of beryllium in the batholith.

We spent one week at the locality in August, 1994. Field activities centred on Mulligan's occurrence, south of the Ice Lakes. A region 6 km by 3 km was investigated, sampled and mapped, and the occurrence of beryllium-bearing pegmatites was delimited (see Groat *et al.* 1995b).

Granitic pegmatites are common in the area; aplite dikes are distinctly less common than the pegmatites. All pegmatites are hosted by the batholith; field relations suggest that the area of investigation represents an upper margin of the batholith. The host granite is variable in texture, ranging from fine-grained to megacrystic and sometimes pegmatoid, and unshattered to distinctly sheared; it shows many of the field characteristics expected of granites parental to pegmatite fields. Pegmatite distribution is zoned; NNE to SSW traverses show the following zonation sequence: pegmatite-free  $\Rightarrow$  barren-pegmatite  $\Rightarrow$  biotite + muscovite-bearing pegmatite  $\Rightarrow$  beryl-bearing pegmatite  $\Rightarrow$  biotite + muscovite-bearing pegmatite. Exposures to the extreme SSW are too poor to trace pegmatite zonation past the last sequence in the zonation scheme. In general, beryllium-enriched pegmatites are localized in a NNW to SSE trending topographic high in this part of the batholith.

Pegmatites are most commonly as dikes, less commonly as irregular pods. They are typically inextensive along strike (<10 m) and less than 0.5 m thick. The pegmatites tend to be well zoned; the usual margin to core sequence is (1) narrow plagioclase-rich border zone, (2) graphic K-feldspar + quartz  $\pm$  2 mica plagioclase wall zone, (3) blocky K-feldspar + quartz intermediate

zone, and (4) a quartz core. Plumose muscovite is sometimes found at the wall zone-intermediate zone contact. Accessory phases include beryl, allanite and magnetite. Cross-cutting relationships indicate the aplite to be younger than the pegmatites.

The Ca content of (rare) garnet from the Ice Lakes pegmatites suggest a higher degree of fractionation than the Horseranch or Cassiar East pegmatites (Fig. 2). The tourmaline geochemistry (Fig. 3) and the K-Rb signature as seen in the feldspars and micas (Fig. 4) suggests an intermediate degree of fractionation.

Beryl crystals range to 5 cm in length, and beryl-bearing pegmatites are common in the area; however, the concentration of beryl in these pegmatite bodies is generally low. Because of the anticipated low grades of beryllium, the deposit is unlikely to be of economic value. Furthermore, while the large tonnage, low-cost Spor Mountain deposit in Utah is in production, (annually supplying approximately 60% of the world's beryllium), North American pegmatitic deposits of beryllium will remain subeconomic.

#### 8. CASSIAR BATHOLITH, EASTERN MARGIN (YT; 60°27'N, 130°40'W)

Poole (1957) describes abundant bodies of granitic pegmatite at the eastern margin of the Cassiar batholith (near Caribou Lake): the quantity of pegmatite varies from zero to nearly 95% at the batholithic contact. We spent more than a week in the area in 1995. Given the results of our work the previous year in the Ice Lakes area we anticipated that these pegmatites would be rare-element-enriched and worthy of our attention.

However, this turned out to not be the case. It took several days to find the pegmatites, all of which are hosted by the batholith. All of the pegmatites were barren and devoid of exotic accessory phases. Electron microprobe analyses of garnets (Fig. 2), tourmalines (Fig. 3), and feldspars and micas (K-Rb signature; Fig. 4) all suggest that these are the most barren (poorly fractionated) pegmatites encountered in our studies.

## 9. CLEA PLUTON, SELWYN PLUTONIC SUITE (YT; 62°46.5'N, 129°52'W)

The Clea pluton is a small (0.3 km<sup>2</sup> in exposure), massive to weakly foliated two-mica granite, and is another member of the Selwyn plutonic suite. It is associated with a tungsten skarn (described by Tompson 1978, and Godwin *et al.* 1980). Anderson (1983) divides this pluton into equigranular and coarsely megacrystic phases. Pegmatite seams and pods intrude both phases and the scheelite-bearing skarns.

We spent one week at the Clea pluton in August, 1994. Three types of marginal to satellitic dikes were observed and sampled: aphanite (alaskite), aplite, and granitic pegmatite dikes. Aphanite and aplite dikes are intersected by hydrothermal quartz veins which host low concentrations of tungsten mineralization. We found pegmatite dikes to be extremely uncommon and small (to 1 m thick). The few dikes exposed in outcrop have irregular contacts, are pod-like in shape, simple in geochemistry and mineralogy (no concentrations of rare metals), and are simply zoned (concentric border, wall, intermediate, and quartz zones). Biotite is the only mica associated with the pegmatite dikes. None of the exposed pegmatite dikes host any W-mineralization or show cross-cutting relationships with hydrothermal veins.

We had hoped that pegmatite would be reasonably abundant or geochemically complex to (1) test models on the timing of pegmatite generation and generation of hydrothermal W mineralization, and (2) assess the economic potential of pegmatite deposits associated with W-mineralized granites of the Yukon. Clea does not provide these answers, and casts an unfavourable light on the economic potential of pegmatites associated with W-mineralized granites and their deposits. It does, however, raise many questions about the timing and role of water saturation in granitic melts parental to rare-metal (Sn, W) hydrothermal deposits.

As all granitic pegmatites hosted by the Clea pluton were barren and devoid of exotic accessory phases, all analytical work concentrated on previously unstudied accessory phases in a number of hydrothermal deposits in and about the pluton (see Groat *et al.* 1995b). Mineral chemistry is, on the whole, unexceptional. Cassiterite is mildly tantalian and titanian, well below extremes shown by granites and associated deposits. Tungsten oxide minerals (scheelite and wolframite) are impoverished in trace HFSE such as Ta and Nb, and show low to moderate Fe/Mn ratios (2.7 in

wolframite). All apatite samples are fluorapatite; Cl is conspicuously absent in these samples, and transition metal contents (*e.g.*, Mn, Fe) of the samples are low. Given the barren pegmatite dikes, the lack of any direct association of pegmatite dikes with hydrothermal deposits, the lack of a common HFSE-bearing accessory mineralogy of pegmatite dikes and hydrothermal deposits, and the unexceptional chemistry of accessory oxides and phosphate minerals in the hydrothermal deposits, little can be said about the relative timing and relationship of pegmatite-generating events and the main hydrothermal event at Clea.

## 10. THE LITTLE NAHANNI PEGMATITE GROUP (NWT; 62°12'N, 128°50'W)

### 10.1 Geological Setting

The granitic pegmatites are located in an unnamed mountain range bound to the northeast by the March Fault and to the southwest by Steel Creek. The dominant structural features of the range are the Fork Anticline and the Summit Syncline, major features of the Selwyn Fold Belt (Gordey & Anderson 1993). The folds trend northwest-southeast, and plunge to the northwest. The pegmatites are localized in the northeast arm to axial sections of the Fork Anticline. In general, they strike northwest; *i.e.*, subparallel to the strike of axial planes of the fold system. They are dominantly hosted by calcareous metasedimentary rocks of the upper Yusezyu Formation, which consist of mildly metamorphosed equivalents of limestone, variably calcareous sandstone and shale. Granitic plutons are unexposed in the vicinity of the pegmatite group. Syntectonic metamorphism in the immediate study area, however, occurred at an anomalously high grade for this region. Andalusite porphyroblasts occur scattered throughout the metasedimentary rocks, and appear to be coarser in areas to the north of the pegmatite group. Late-tectonic porphyroblasts of staurolite and cordierite, and chlorite pseudomorphs after garnet (?), indicate that the area experienced syntectonic metamorphism at temperatures in excess of 500°C. This may reflect the existence of a pluton at shallow levels below the present erosional surface.

### 10.2 Description of the Pegmatites

*Field Relations.* The pegmatites range from tabular to lenticular in shape. They have high aspect ratios; individual dikes are a maximum of a few meters in width yet can extend for several

kilometers along strike. Contacts are typically sharp, sometimes irregular depending upon the type of host rock. Pegmatites emplaced in calcareous metasedimentary rocks show low degrees of assimilation as evidenced by calcite-lined fractures and late calcium-rich mineral assemblages (often including apatite). Pegmatites emplaced in pelitic metasedimentary rocks often have wide (up to 10 cm) exomorphic aureoles rich in coarse silvery mica or narrow (several mm) bands of black tourmaline. The pegmatites show no mineralogically obvious signs of regional zoning over the 10 km extent of the group.

The pegmatites appear to be synchronous to late in the timing of the last tectonic event to affect the region: dike attitude and shape is variable, ranging from moderately-dipping, contorted and conformable to sedimentary layering to sub-vertical, tabular, undeformed and cross-cutting host strata. The pegmatite group is lithium-rich; the mineralogy and style of internal zoning indicates the group to belong to the albite-spodumene type of the rare-element class of granitic pegmatites (Cerny 1991).

*Mineralogy and Internal Zoning.* The dominant minerals of the pegmatite dikes are quartz, potassium feldspar, and albite. Subordinate to these are spodumene, then lepidolite, the dominant carriers of lithium. The spodumene seems to contain trace quantities of manganese, as evidenced by the pink colour of weathered samples, and by the concentration of black manganese oxides along fracture planes. Spodumene and K-feldspar are typically the coarsest phases, with individual crystals often greater than 10 cm in length, and account for the pegmatitic texture of most dikes. Albite is variable in size and texture; mostly it is saccharoidal in texture, but in places is coarsely cleavelanditic. Lepidolite is similarly variable, comparable in size to saccharoidal albite in aplitic sections of dikes, but ranging to coarse-grained "ball-peen" (colliform) lepidolite in pegmatitic sections of some dikes. Accessory minerals include tantalian rutile and cassiterite, columbite-group minerals, Mn-bearing apatite, lithiophilite, amblygonite-montebasite, and beryl. Electron microprobe work shows that many of the oxide phases are strongly oscillatory zoned.

Internal zoning of the pegmatites ranges from simple to chaotic. Where simple, the outward to inward succession of zones consists of a narrow border unit, one to two wall units, an irregularly-zoned intermediate unit, and uncommonly, a quartz core. Where chaotic, there is less of a distinction between wall and intermediate units as expressed by alternations of aplitic and

pegmatitic layers. At contacts there is a thin fine-grained border unit rich in plagioclase and muscovite. The wall unit dominantly consists of plagioclase and quartz, with lesser amounts of K-feldspar. Pegmatites emplaced in pelitic metasediments have two wall units, the outermost of which has relatively higher concentrations of muscovite or lepidolite. Wall units vary considerably in thickness and texture but are typically several cm in width and aplitic in texture. The contact between the wall unit and the intermediate unit is not sharp, but is defined by a coarsening of mineral textures towards the centres of dikes. For many dikes, the first appearance of spodumene can be used as a reliable indicator of the start of the intermediate unit. In general, the intermediate unit consists of K-feldspar, plagioclase, quartz, spodumene, with or without lepidolite. The appearance or absence of lepidolite can simply be explained as being due to slight variations in  $m$  HF, pushing phase relations in and out of the lepidolite-stable field (London 1984). The intermediate unit is typically rhythmically banded; this banding is expressed in two ways: (1) as alternations of pegmatitic and aplitic layers, and (2) as variations in modal mineralogy of aplitic layers. Aplitic layers are similar in mineralogy and texture to the wall unit. Pegmatitic layers consist of coarse-grained K-feldspar, spodumene, and quartz with or without lepidolite. Directional crystal growth is strongly expressed by (1) banding in the aplitic layers, which is parallel to dike contacts, and by (2) elongate K-feldspar and spodumene crystals in the pegmatitic layers, which are perpendicular to dike contacts. Monomineralic quartz cores are rare and occupy central portions of the dikes.

*Geochemistry and Petrogenesis.* The pegmatite dikes are peraluminous. The dikes show an overall predominance of lithophile elements; they are strongly enriched in lithium and fluorine, weakly enriched in phosphorus, manganese, beryllium, tantalum, and niobium. The absence of tourmaline (except at exocontacts) indicates that the pegmatites are poor in boron. Microprobe analyses of oxide phases show that the dikes are enriched in Mn with respect to Fe, and in Ta with respect to Nb (Groat *et al.* 1994, 1995a, 1995b). Thus, in terms of mineralogy and preliminary geochemistry, the group is part of the LCT (*Li-Cs-Ta*) geochemical suite of granitic pegmatites (Cerny 1991). The sporadic occurrence of goshenite beryl implies a possible Cs enrichment.

Electron microprobe analyses show that the Ca content of garnet is an indicator of degree of fractionation (Fig. 2a). However, the high Ca concentration in the LNPG garnets is anomalous, and is most likely due to the assimilation of limestone (the garnets most often occur in calcite-lined



fissures in the host pegmatite dikes). Note that the covariance of Mg with Fe/Mn (Fig. 2b) is relatively poor. This is probably due to competition between garnet, micas, and tourmaline for Mg. The corresponding graph for tourmaline (Fig. 3b) shows a more consistent trend.

Electron microprobe analyses of the feldspars and micas indicate that the Group is highly evolved in terms of K-Rb systematics (Fig. 4). Note that in terms of K/Rb fractionation, all other pegmatite groups are intermediate, with the exception of pocket minerals in Li-dikes of O'Grady which attain levels similar to the LNPG. However, it is interesting to note that the LNPG is much less evolved than O'Grady in terms of K-Cs systematics.

Phase relations amongst the lithium aluminosilicates can be used to apply preliminary petrogenetic constraints to pegmatite evolution (London 1984). The absence of (1) primary petalite, (2) secondary spodumene plus quartz intergrowths, and (3) eucryptite, in the presence of primary spodumene plus quartz, implies relatively low T/moderate P emplacement conditions for the pegmatitic melts (*circa* 3 to 3.5 kb, 550-650°C).

### 10.3 Geochronology

The details of the geochronology study are given in Mauthner *et al.* (1995). Columbite, muscovite, and lepidolite were used because of the absence of zircon, titanite, and monzonite. Cassiterite was not used because of abundant inclusions. A U-Pb age of  $81.6 \pm 0.5$  Ma was obtained for columbite. K-Ar ages for micas were determined to be  $65.4 \pm 4.0$  Ma for muscovite, and  $65.8 \pm 3.4$  Ma and  $65.4 \pm 3.6$  Ma for lepidolite. The U-Pb ages are interpreted to be the emplacement date for the pegmatites and the K-Ar ages are interpreted to be the timing of a thermal event responsible for resetting the K-Ar mica system. The U-Pb columbite ages are 8 to 13 Ma younger than the average age of the plutons in the Selwyn plutonic suite and indicate that these pegmatites represent a magmatic event that has not been previously recognized. Likewise, the K-Ar ages point to a later thermal event not previously recognized in this area.

## 11. THE O'GRADY BATHOLITH (NWT; 62°45' to 63°N, 128°30' to 129°15'W)

The O'Grady batholith is located in the western Northwest Territories, approximately 100 km NNW of Tungsten, in the Selwyn Mountains. Our decision to investigate the batholith was prompted by information in Gordey & Anderson (1993). They reported that it is a 270 km<sup>2</sup> hornblende-bearing, alkali-feldspar-rich composite intrusion with S-type characteristics, consisting of a megacrystic hornblende quartz syenite core, a marginal massive equigranular hornblende-biotite granodiorite, and a foliated transitional phase between the two.

We spent a week on the western margin of the O'Grady batholith in August 1994. We found abundant pegmatite and aplite dykes along the margin, especially in the outer parts of the quartz syenite core. We returned to the batholith in the summer of 1995 to determine the extent of the pegmatite-rich area, and discovered that it is much smaller (about 5 km<sup>2</sup>, at approximately 62°53'N, 128°59'W; see Figure 5) than the "zone of common leucocratic aplite, pegmatite, and alaskite intrusions" shown in Gordey & Anderson (1993).

The quartz syenite host is remarkably homogeneous over the investigated region; the only obvious field variation is in the modal abundance of hornblende. Aplite dykes show uniform characteristics: fine-grained, plagioclase-feldspar-rich, moderately boron-rich (abundant tourmaline). The dykes are typically small (1 m to, exceptionally, a few m in width), and often occur in en-echelon swarms.

The vast majority of granitic pegmatites are coarse-grained (crystal size often exceeds 10 cm) and rich in B, as shown by abundant tourmaline and sporadic axinite. Most of the pegmatites show simple internal zonation; the typical margin-to-core sequence is: a border unit (feldspar-rich), followed by a wall unit (graphic K-feldspar + quartz ± plagioclase feldspar), an intermediate unit (blocky K-feldspar, quartz) and a quartz core. The intermediate unit and the quartz core are commonly miarolitic. Most of the pegmatites show a distinct NYF affinity, hosting magnetite, allanite, titanite, amazonite, and some smoky quartz. However, pegmatites near the upper margins of the batholith show LCT characteristics in the form of lepidolite, gem-quality coloured tourmaline, and rare boro- and beryllosilicate minerals.

Note that the Li-enriched and Li-poor pegmatites are co-eval. Both show abundant tourmaline and amazonite and similar gross characteristics (*i.e.*, shape, size, textural properties). The Li-enriched pegmatites do not represent a separate (*i.e.*, later) generation. The O'Grady pegmatites could be thought of as transitional to the NYF (Li-poor dykes) and LCT types (Li-bearing dykes).

Satellitic dykes on the western margin of the batholith were also investigated (in 1994). We had anticipated that such dykes would represent exterior pegmatites (*i.e.*, exterior to the O'Grady batholith), which, according to current prospecting models for pegmatite deposits, should be more rare-metal-enriched than the interior to marginal pegmatites. All investigated satellitic dykes are aphanitic in texture (*i.e.*, non-pegmatitic). By inference, either exterior pegmatite dykes are absent (*i.e.*, perhaps the finer-grained marginal phases of the batholith were impermeable to pegmatitic melts, thus trapping the pegmatites within the confines of the current-day batholith), or all significant migration of pegmatite melts was upward, and erosion has removed all traces of resultant dykes.

### 11.1 Mineral Chemistry

*Tourmaline.* Most analytical work focused on variations in tourmaline chemistry, as tourmaline is the main indicator of Li enrichment in the dykes. Selected aspects of tourmaline geochemistry are shown as a function of the fractionation indicator  $Mn/(Mn + Fe)$  in Figure 6. Samples with  $Mn/(Mn + Fe)$  less than 0.05 represent dykes which host only schorl; samples with  $Mn/(Mn + Fe)$  greater than this value represent Li-enriched dykes which host coloured tourmaline (elbaite)  $\pm$  lepidolite. Consistent behaviour is shown by tourmaline samples from the various dykes: Mn, F, and Li behave incompatibly (increase with fractionation), and Fe, Ti, and Mg behave strongly compatibly (decrease with fractionation). These are normal trends for LCT-class granitic pegmatites. The high degree of correlation of  $F/(F + OH)$  with incompatible cation concentrations may indicate that incompatible metals are complexed with fluorine in the melt (*cf.* Keppler 1993).

Tourmaline chemistry of samples from the O'Grady batholith pegmatites and other pegmatite groups from the northern Cordillera is shown in Figures 3a and b. The graphs show that  $F/OH$  increases and  $Fe/Mn$  decreases with fractionation. Note the very broad range for O'Grady; the

schorls extend to much lower degrees of Fe/Mn fractionation (*i.e.*, larger values) than other localities, and the elbaïtes are extremely enriched in F relative to OH and are depleted in Mg.

One conclusion we can make is that tourmaline colour is a useful indication of Li enrichment (black is Li-poor, coloured varieties are Li-rich), however, for low to moderate degrees of Li enrichment, colour changes may not be visible in hand specimen or even in thin section. Diagrams like Figure 4a may help with assessing the Li potential within and between pegmatite populations. Note, however, that some tourmaline crystals from the O'Grady pegmatites show compositional zoning.

*Feldspar.* Most plagioclase in the dykes is extremely sodic, with compositions ranging from  $An_0$  to  $An_4$  (analyses F16-19, lamellae associated with K-feldspar, and analyses F24-26). However, a sample of oligoclase (var. cleavelandite) with composition  $An_{30}$  (analysis F27) was found in a pegmatite dike. K-feldspar (analyses F1-7) is only weakly to moderately enriched in large-ion lithophile elements. The analyses indicate that samples from Li-enriched dykes are more enriched in LILE (Rb, Cs) than samples from Li-poor dykes. K/Rb ratios for K-feldspar are not exceptional. They range from 327 (microperthite matrix, pegmatite dike) to 61 (cryptoperthite matrix, Li-enriched pegmatite dike), somewhat outside the range shown by the batholith ( $151 \pm 24$ , Gordey & Anderson 1993), and typical of moderately-lithophile-fractionated pegmatite dykes (Cerny 1991).

The K/Rb ratios are plotted against wt.% Rb in Figure 4a for K-feldspar samples from the O'Grady batholith pegmatites and from other pegmatites in the northern Cordillera. Cassiar East represents a barren pegmatite group, and shows a primitive K-Rb signature. The feldspars on the LNPG indicate that it is highly evolved in terms of K-Rb systematics. The other pegmatite groups are intermediate in terms of the K-Rb system.

*Mica.* Lepidolite is the second-most abundant carrier of Li in these dykes, and is recognized by its characteristic violet colour. As a species, lepidolite can show a broad range of Al:Li ratios. The analyzed samples (M1-3; lepidolite from a Li-enriched pegmatite dike, cirque 3) show high degrees of Li enrichment, and are moderately enriched in Cs [K/Cs = 26 (M1), 8 (M2), 6 (M3)],

reflective of its late timing in the crystallization history of the Li-enriched pegmatite dykes (always as a pocket phase).

A plot of K/Rb ratios *versus* wt.% Rb for the micas (Figure 4b) is very similar to that for K-feldspars. Note, however, that the pocket lepidolites from Li-enriched dykes of the O'Grady batholith show levels of K/Rb fractionation similar to the LNPG. It is interesting to note that O'Grady is much more evolved than the LNPG in terms of K-Cs systematics; this is shown by the occurrence of a Cs-analogue of lepidolite, and the elevated Cs content of feldspars and micas (this is not shown in a plot because most localities other than O'Grady have undetectable Cs).

Analysis M4 is of an unknown nanpingite  $[\text{CsAl}_2(\text{Si,Al})_4\text{O}_{10}(\text{OH,F})_2]$ -lepidolite-like late green mica from a Li-enriched pegmatite dike in cirque 3. The analysis is not included in Figure 4b because Cs no longer behaves like a trace- to minor-element in this mineral; its K-Rb systematics deviate from the norm for micas.

*Allanite.* As noted previously, allanite is an uncommon constituent in the pegmatites. When present it often shows oscillatory zoning due to variations in REE content.

*Axinite.* Axinite is low in abundance in all dykes, but occurs in many dykes in the area. Axinite is recognized by its euhedral, bladed crystals, and pale violet-grey colour. The presence of axinite in conjunction with tourmaline indicates that the dykes show high degrees of B enrichment. The analyzed sample (analyses AX1-5) comes from a schorl-bearing (pegmatite) dyke and, like schorl, shows high degrees of Fe enrichment.

*Danburite.* A sample of danburite (analysis D1) was found in a pocket in a Li-enriched pegmatite dyke (cirque 3).

*Hamborgite.* Hamborgite is the sole concentrator of Be in the dykes. It is rare, found only in the most fractionated Li-enriched dykes. Only moderate enrichment in F *versus* OH is shown by the analyzed sample (analysis H1, of an inclusion in an elbaite crystal from a pocket in a Li-enriched dyke in cirque 3).

*Opal.* Opal showing compositional zoning is also associated with the pegmatites.

*Titanite.* Titanite samples show low to moderate degrees of enrichment in Ta and Nb (to 2.3 wt.% Nb<sub>2</sub>O<sub>5</sub> + Ta<sub>2</sub>O<sub>5</sub>) and moderate to high degrees of enrichment in F (to 1.25 wt.% F; see analyses TT1-9, all from pegmatite dykes). These points are consistent with other data for the dykes, indicating the pegmatite melts to be F-rich, yet conspicuously poor in HFSE such as Ta, Nb, Sn or W.

*Zircon.* Only one zircon crystal was analyzed (analyses Z1-4, from a pegmatite dyke). The results are shown in Figure 7, a plot of zircon geochemistry as a function of U/(U + Th) and mineral zonation. The zircon sample is enriched in U, Th, Y + HREE, and moderately to weakly enriched in Hf. Core to rim zonation shows that (1) crystal-melt systematics were not sufficient to result in significant Zr-Hf fractionation, (2) total actinide element content diminishes with increasing U-Th fractionation, and (3) Y + HREE behave compatibly.

## 11.2 Whole-Rock Geochemistry

Whole-rock analyses of the quartz syenite host were done by Chemex Labs Ltd. and are given in Appendix 2. The rock is geochemically unspectacular. The K/Rb ratio (K by ICP) is 152 or 131 (depending on technique), which is inside the range (151 ± 24) given by Gordey & Anderson (1993). The K/Cs ratio (2249) indicates that the Cs content of the host rock is much lower than in some micas and feldspars from Li-enriched pegmatites.

## 11.3 Origin of the Li-Enriched Pegmatites

From a geochemical viewpoint, the association of Li-enriched pegmatite dykes with the O'Grady batholith is highly unusual. Previous work has indicated the batholith to show only low degrees of fractionation: it is at most metaluminous, the most fractionated unit of the batholith is a hornblende-bearing quartz syenite, and trace-element chemistry is unexceptional (Gordey & Anderson 1993). The question exists as to how Li enrichment came about: by extreme fractionation of a rather unexceptional parent, or by assimilation of Li- and B-enriched overlying metasediments. The coincidence of Li and B enrichment, the localized occurrence of Li-enriched

dykes, and the geochemical unsuitability of the quartz-syenite host to the dykes as an immediate parent to Li and B-enriched pegmatite dykes could be cited as supporting an assimilation origin. However, the high Li and Rb, Cs contents of the elbaite-bearing pegmatites indicates that these pegmatites formed by fractionation, not by assimilation of Li-rich metasediments. It is still difficult to conceive of a magma now represented by the hornblende quartz syenite as directly generating dykes of these compositions by fractionation. Instead, a more evolved (direct) parent is called for. Further, as field relations imply that current erosional levels for the batholith are near the upper margin, the chances seem good for other (*i.e.*, more evolved) phases of the batholith below the current erosional surface.

## 12. PROSPECTING FOR RARE-ELEMENT BEARING PEGMATITES

In terms of prospecting for rare-element pegmatites, the previous section reinforces the importance of the following indicators of fractionation:

1. Mineralogical diversity. In short, the more diverse the mineral assemblage, the more fractionated the pegmatite, and the better the economic target.
2. Occurrence of rare-element indicator minerals (columbite, beryl, spodumene, lepidolite, coloured tourmaline, nanpingite, etc.).
3. Geochemical enrichment, monitored using (a) fractionating element pairs (Fe/Mn, Nb/Ta, etc.); (b) compatible/incompatible element variations (compatible: Ba, Mg, Ti, etc.; incompatible: Rb, Li, Cs, etc.); (c) isotope geochemistry, *e.g.* Sr ratios (the more radiogenic, the better).

Another point to be made is that when the "parent" plutons are exposed (as at O'Grady, Horseranch, possibly Ice Lakes, the Seagull batholith) we seem to be observing their upper margins. What is unusual is that there are no horizontal pegmatite halos around the batholiths. In the case of the LNPG there is a well-exposed pegmatite group, but the granite is at depth. It seems unusual that there are no crustal sections with granites and (exterior) pegmatites exposed. This may be because all pegmatite melt migration in the Selwyn plutonic suite is upwards relative to the location of the parental granite. If this is the case, locating (exposed) radiogenic granites may not

be a good strategy for locating pegmatite fields. Instead the best strategy may be to initially use dense populations of radiogenic granites/granitoids as an indication of broad areas where pegmatites are likely to be found. After that it may be necessary to use geochemical sampling to locate anomalies (especially of Li).

Most of the pegmatites we have seen are interior pegmatites. Where are the exterior pegmatite groups? Is the LNPG the only example of exterior pegmatites? It could be that we are looking at granites emplaced at high crustal levels (i.e. in relatively cool hosts; note that the regional metamorphic grade is low). The cool ambient conditions of the country rocks coupled with the development of chilled margins for the granitoids may have prevented pegmatite melts from migrating far from their source. If this is the case, the LNPG is an anomaly. It might be that the presence of staurolite in the host rocks and the presence of spodumene in the pegmatites indicates that the mountain range hosting the LNPG represents a deeper crustal section than surrounding parts of the Selwyn Mountains. More work needs to be done in the area to answer these questions.

### 13. SCIENTIFIC COMMUNICATIONS

#### 13.1 Refereed Journal Publications

Mauthner, M.H.F., Mortensen, J.K., Groat, L.A. & Ercit, T.S. (1996): Geochronology of the Little Nahanni Pegmatite Group, Selwyn Mountains, southwestern Northwest Territories. *Can. J. Earth Sci.* **32**.

A paper on the mineralogy and geochemistry of the O'Grady pegmatites is in preparation, and will be submitted to *Canadian Mineralogist* in late summer (1996).

#### 13.2 Refereed Conference Abstracts

Groat, L.A. & Ercit, T.S. (1996): Granitic pegmatites of mixed NYF-LCT affinity from the O'Grady batholith, NWT. *Geol. Assoc. Can./Mineral. Assoc. Can. Program & Abstr.* **21**, A-38.



- Ercit, T.S., Groat, L.A., Mauthner, M.H.F. & Raudsepp, M. (1996): Regional versus local variations in the geochemistry of Ta-Nb oxide minerals: Little Nahanni Pegmatite Group. *Geol. Assoc. Can./Mineral. Assoc. Can. Program & Abstr.* **21**, A-26.
- Mauthner, M.H.F., Groat, L.A., Mortensen, J.K., Raudsepp, M. & Ercit, T.S. (1995): The Little Nahanni Pegmatite Group, Northwest Territories, Canada: An albite-spodumene type pegmatite. *Geol. Soc. Am. Abstr. & Programs* **27**, A-411.
- Raudsepp, M., Mauthner, M.H.F., Groat, L.A. & Ercit, T.S. (1995): Characterization of phosphate minerals in albite-spodumene pegmatites of the Little Nahanni Pegmatite Group, Northwest Territories. *Geol. Soc. Am. Abstr. & Programs* **27**, A-471.
- Mauthner, M.H.F., Mortensen, J.K., Groat, L.A. & Ercit, T.S. (1995): Geochronology of the Little Nahanni Pegmatite group and implications for regional tectonics. *Geol. Assoc. Can./Mineral. Assoc. Can. Program & Abstr.* **20**, A-67.
- Mauthner, M.H.F., Groat, L.A., Ercit, T.S., Mortensen, J.K. & Raudsepp, M. (1994): Mineralogy, geochemistry, and geochronology of the Little Nahanni Pegmatite Group, Northwest Territories, Canada. *Geol. Soc. Am. Abstr. & Programs* **26**, A-222.
- Groat, L.A., Ercit, T.S., Raudsepp, M., Mauthner, M.H.F. & Ahlborn, V. (1994): Geology and mineralogy of the Little Nahanni Pegmatite Group. *Geol. Assoc. Can./Mineral. Assoc. Can. Program & Abstr.* **19**, A-26.

#### 14. BENEFIT TO THE YUKON TERRITORY

Since 1992 we have spent approximately \$172,000 on field work in northwestern Canada. Support was obtained from the Yukon MDA (\$51,000), Canamera Geological Limited (estimated \$50,000), the Canadian Museum of Nature (\$24,000), DIAND Yellowknife (\$24,000), and NSERC Research Grants to LAG and M. Raudsepp (\$23,000). Almost all of this money was spent in the Yukon Territory, primarily in Watson Lake, Whitehorse, and Ross River.

As noted in a previous report (Groat *et al.* 1995a) the entire LNPG area (35 km<sup>2</sup>) was staked by Canamera Geological Limited of Vancouver. This was done on the basis of our research but without our knowledge. The company is continuing to develop the property for its Li, Ta, Nb, and Be potential.

As noted in Groat *et al.* (1995a), the gem tourmaline from the Li-enriched pegmatites of the O'Grady batholith is of cutting grade. The area was staked in early 1996 by Alpine Gems Limited. The company is planning to develop the property, beginning this summer (1996) with a program of mapping, drilling, and blasting.

## 15. SUGGESTIONS FOR FUTURE WORK

There are a number of areas that we identified to be of interest that we have been unable to visit. These areas should be looked at in the future to assess their pegmatite potential. The areas are listed below.

### 15.1 Seagull Batholith (YT: 60°10'N, 131°30'W)

The Seagull batholith is a medium-sized (300 km<sup>2</sup>) mid-Cretaceous meta- to peraluminous leucocratic granite; with an initial <sup>87</sup>Sr/<sup>86</sup>Sr ratio of 0.7120 (Mato *et al.* 1983). As described by Sinclair & Richardson (1992) it contains quartz-tourmaline orbicules that appear to be the product of a hydrous, B-, F- and Fe-bearing fluid that was trapped in a crystallizing granitic melt. Anomalous concentrations of Sn (12 to 90 ppm) in the orbicules suggest that this fluid may have been related to the hydrothermal fluids that formed Sn-bearing veins and skarns associated with the Seagull batholith (described by Mato *et al.* 1983, and others).

The Seagull batholith has relatively high contents of lithophile elements such as Li, Be, Nb, Rb and Ga; F contents range from 0.15 to 0.65%, significantly higher than those of most other granitic rocks (Sinclair & Richardson 1992).

### 15.2 Thirtymile Pluton and Ork Stock (YT; 60°45'N, 132°15'W)

As described by Liverton (1990), the Thirtymile pluton is roughly elliptical in shape, with a diameter of 8 km. It is made up of four facies: a porphyry, an equigranular microgranite, a megacrystic granite, and a leucocratic topaz- and fluorite-bearing microgranite. The latter contains pale, lithium mica as a major component. Topaz is a common interstitial mineral; fluorite is also common. Tourmaline, apatite, and allanite are occasional accessories. The nearby Ork stock is similar to this facies of the Thirtymile pluton.

### 15.3 Mount Mye Batholith, Anvil Plutonic Suite (YT; 62°20'N, 133°15'W)

As described by Pigage & Anderson (1986), the Mount Mye batholith of the Anvil plutonic suite, near Faro) is a heterogeneous, peraluminous two-mica granite of mid-Cretaceous age (initial  $^{87}\text{Sr}/^{86}\text{Sr} = 0.7405$ ) that falls within the modal field for granites of the Selwyn suite. However, it is not analogous to the highly-evolved, lithophile-element-enriched siliceous plutons of the Selwyn suite, and therefore may have limited potential as a precursor to rare-element enriched pegmatites.

### 15.4 Lened, CAC, and RUDI Plutons (NWT; 62°20-25'N, 128°30-40'W)

These plutons are small, massive, composite stocks associated with important tungsten skarns (Dick 1980). Leucocratic granitic aplite dikes and tourmaline-bearing pegmatite dikes are associated with the plutons. Biotite granite intrusions invade pelitic and calc-silicate hornfels near the CAC and RUDI plutons. They contain muscovite, garnet, andalusite and tourmaline, and some are miarolitic. These peraluminous dikes seem to be characteristic of plutons with extensive tungsten skarns (Anderson 1982).

### 15.5 Sekwi Mountain Map Area (YT/NWT; near MacMillan Pass)

A hornblende-absent, biotite bearing pluton has been reported from this area (Anderson 1983); little is known about it.

### 15.6 Macmillan Pass (YT/NWT; Mactung)

At Mactung, the highest ore grades are associated with zones where quartz veins and aplite and pegmatite dikes are the most abundant, south of the southern margin of the pluton (Atkinson & Baker 1983).

### 15.7 Mid-Cretaceous Suite, Intermontane Belt (YT; 60°40'N, 134°10'W)

Morrison *et al.* (1979) mentions stocks, plugs, and dikes of pegmatitic syenite northeast of Marsh Lake in the Whitehorse map area. The syenite occurs within plutons of the mid-Cretaceous suite in the Intermontane Belt, and as isolated masses in the country rock. However, all initial  $^{87}\text{Sr}/^{86}\text{Sr}$  ratios reported by Morrison *et al.* (1979) for the Whitehorse map area are  $< 0.7070$ .

### 15.8 Emerald Lake (YT; 63°36'N, 131°17'W)

In an assessment report by Robertson *et al.* (1981) the Emerald Lake intrusion is described as an elongate, east-west trending body approximately 12 km long and 1.5 to 2.0 km wide. It is primarily syenitic in composition and presumably of Cretaceous age. One part of the intrusion contains a number of very large vugs consisting of large crystals of smoky quartz in a matrix of highly weathered feldspar and mica with minor amounts of arsenopyrite and unidentified minerals believed to be Au-Ag tellurides. Other features indicative of late-stage fluids within the intrusion are the large miarolitic cavities. These range from "incipient vugs" of 10 to 20 cm in diameter to true miarolitic cavities up to 1.5 m in diameter (but 4 m or more in length where they occur as "swells" on a vein) containing quartz crystals up to 1 m in length, tourmaline and mica. In several areas, well-defined vein systems (seen on cliffs, and described as pegmatites on the map in Robertson *et al.* 1981) end abruptly and are replaced by a zone of cavities.

## 15. ACKNOWLEDGEMENTS

Financial support for the 1995 program was provided by Canamera Geological Limited, the Canada/Yukon Mineral Development Agreement (Whitehorse), the Department of Indian Affairs and Northern Development (Yellowknife), by the Natural Sciences and Engineering Research

Council of Canada in the form of a Research Grant to LAG, and by the Canadian Museum of Nature in the form of an RAC Research Grant to TSE.

## 16. REFERENCES

- Anderson, R.G. (1982): Geology of the Mactung pluton in Niddery Lake map area and some of the plutons in Nahanni map area, Yukon Territory and District of Mackenzie. *In Current Research, Part A. Geol. Surv. Can., Pap. 82-1A*, 299-304.
- Anderson, R.G. (1983): Selwyn plutonic suite and its relationship to tungsten skarn mineralization, southeastern Yukon and District of Mackenzie. *In Current Research, Part B. Geol. Surv. Can., Pap. 83-1B*, 151-163.
- Anderson, R.G. (1988): An overview of some Mesozoic and Tertiary plutonic suites and their associated mineralization in the northern Cordillera. *In Recent Advances in the Geology of Granite-Related Mineral Deposits* (R.P. Taylor & D.F. Strong, eds.). *Can. Inst. Min. Metall., Spec. Vol. 39*, 96-113.
- Armstrong, R.L. (1988): Mesozoic and early Cenozoic magmatic evolution of the Canadian Cordillera. *In Processes in Continental Lithosphere Deformation* (S.P. Clark, Jr., B.C. Burchfiel and J. Suppe, eds.). *Geol. Soc. Am. Spec. Pap. 218*, 55-91.
- Atkinson, D. & Baker, D.J. (1983): Recent developments in the geologic picture of Mactung: CIM, Mineral Deposits of Northern Cordillera Symposium, 27 (abstr.).
- Cerny, P. (1991): Rare-element granitic pegmatites. I. Anatomy and internal evolution of pegmatite deposits. *Geosci. Can.* 18, 49-67.
- Dick, L.A. (1980): *A Comparative Study of the Geology, Mineralogy and Conditions of Formation of Contact Metasomatic Mineral Deposits in the Northeastern Canadian Cordillera*. Ph.D. thesis, Queen's Univ., Kingston, Ontario.
- Godwin, C.I., Armstrong, R.L. & Tompson, K.M. (1980): K-Ar and Rb-Sr dating and the genesis of tungsten at the Clea tungsten skarn property, Selwyn Mountains, Yukon territory. *Can. Inst. Min. Metall., Bull.* 73, 90-93.

- Gordey, S.P. & Anderson, R.G. (1993): Evolution of the northern Cordilleran miogeocline, Nahanni map area (1051), Yukon and Northwest Territories. *Geol. Surv. Can., Mem.* 428.
- Groat, L.A., Ercit, T.S., Raudsepp, M. & Mauthner, M.H.F. (1994): Geology and mineralogy of the Little Nahanni Pegmatite Group. *Dep. Indian & Northern Affairs, Doc.* EGS 1994-14.
- Groat, L.A., Ercit, T.S., Mortensen, J.K. & Mauthner, M.H.F. (1995a): Granitic pegmatites in the western Northwest Territories. *Dep. Indian & Northern Affairs, Doc.* EGS 1995-?
- Groat, L.A., Ercit, T.S., Mortensen, J.K. & Mauthner, M.H.F. (1995b): Granitic pegmatites in the Canadian Cordillera: Yukon and Northwest Territories. *Dep. Indian & Northern Affairs, Open File* 1995-14 (G).
- Groat, L.A. & Ercit, T.S. (1996): Granitic Pegmatites of mixed NYF-LCT affinity from the O'Grady batholith, western Northwest Territories. *Dep. Indian & Northern Affairs, Doc.* EGS 1996-?
- Kepler, H. (1993): Influence of fluorine on the enrichment of high field strength trace elements in granitic rocks. *Contrib. Mineral. Petrol.* 114, 479-488.
- Liverton, T. (1990): Tin-bearing skarns of the Thirtymile Range: a progress report. *In* Yukon Geology, vol. 3, Exploration and Geological Services Division, Yukon Territory, Department of Indian and Northern Affairs, 52-70.
- London, D. (1984): Experimental phase equilibria in the system  $\text{LiAlSiO}_4\text{-SiO}_2\text{-H}_2\text{O}$ : a petrogenetic grid for lithium-rich pegmatites. *Am. Mineral.* 69, 995-1004.
- Mato, G., Ditson, G. & Godwin, C. (1983): Geology and geochronometry of tin mineralization associated with the Seagull batholith, south-central Yukon Territory. *Can. Inst. Min. Metall., Bull.* 76, 43-49.

- Mauthner, M.H.F., Mortensen, J.K., Groat, L.A. & Ercit, T.S. (1996): Geochronology of the Little Nahanni Pegmatite Group, Selwyn Mountains, southwestern Northwest Territories. *Can. J. Earth Sci.* **32**.
- Morrison, G.W., Godwin, C.I., and Armstrong, R.L. (1979): Interpretation of isotopic ages and initial  $^{87}\text{Sr}/^{86}\text{Sr}$  ratios for plutonic rocks in the Whitehorse map area, Yukon. *Can. J. Earth Sci.* **16**, 1988-1997.
- Mulligan, R. (1968): Geology of Canadian beryllium deposits. *Geol. Surv. Can., Econ. Geol. Rept.* **23**,
- Pigage, L.C. & Anderson, R.G. (1986): The Anvil plutonic suite, Faro, Yukon Territory. *Can. J. Earth Sci.* **22**, 1204-1216.
- Poole (1957): GSC Map 22-1957.
- Robertson, R.C.R., Doherty, R.A. & Garagan, T. (1981): Assessment report for Ice Claims; AGIP Canada Ltd.
- Sinclair, W.D. & Richardson, J.M. (1992): Quartz-tourmaline orbicules in the Seagull batholith, Yukon Territory. *Can. Mineral.* **30**, 923-936.
- Tompson, K.M. (1978): *Geology of the Clea Tungsten Deposit, Yukon Territory*. B.Sc. thesis, Univ. of British Columbia, Vancouver, British Columbia.
- White, A.J.R. & Chappell, B.W. (1983): Granitoid types and their distribution in the Lachlan Fold Belt, southeastern Australia. In *Circum-Pacific Plutonic Terranes* (J.A. Roddick, ed.). *Geol. Soc. Am. Mem.* **159**, 21-34.



## LIST OF FIGURES

Fig. 1. Location map.

Fig. 2. Garnet chemistry of samples from pegmatite groups in northwestern Canada.

Fig. 3. Tourmaline chemistry of samples from pegmatites in the northern Cordillera. Note that in (a) the data for samples with undetected F are plotted at the detection limit for F (at  $F/OH = 0.1$ ). A log-log plot was not used for (b) because the data are linear, and such a plot would exaggerate the area near the origin where analytical problems exist (*i.e.*, it is close to detection limit, poor count statistics, etc.)

Fig. 4. K/Rb ratios versus wt. % Rb for (a) K-feldspar and (b) mica samples from the O'Grady batholith pegmatites and from other pegmatites in the northern Cordillera.

Fig. 5. Sketch map of the O'Grady batholith, showing the zone of Li-enriched pegmatites (adapted from Gordey & Anderson 1993).

Fig. 6. Tourmaline chemistry as a function of the fractionation indicator  $Mn/(Mn + Fe)$ .

Fig. 7. Zircon chemistry as a function of  $U/(U + Th)$  and mineral zonation.

Fig. 1

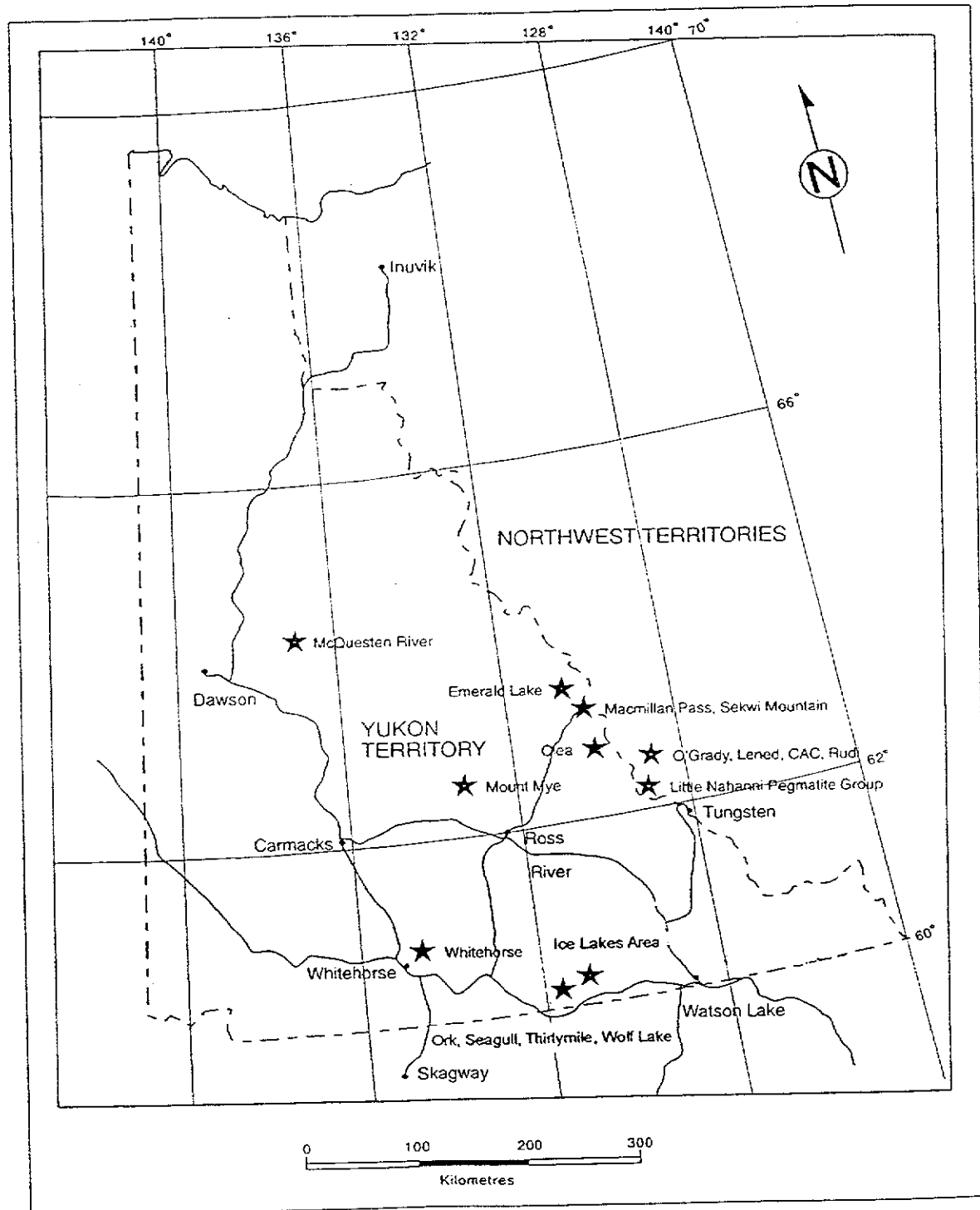


Fig. 2a (left), 2b (right)

Garnet

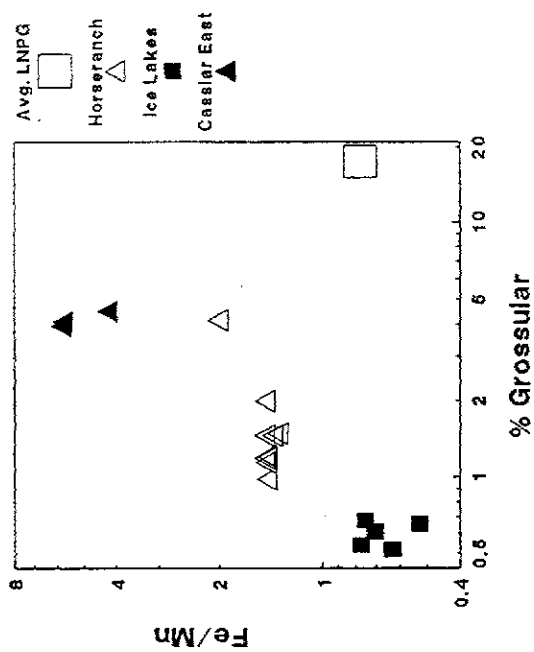
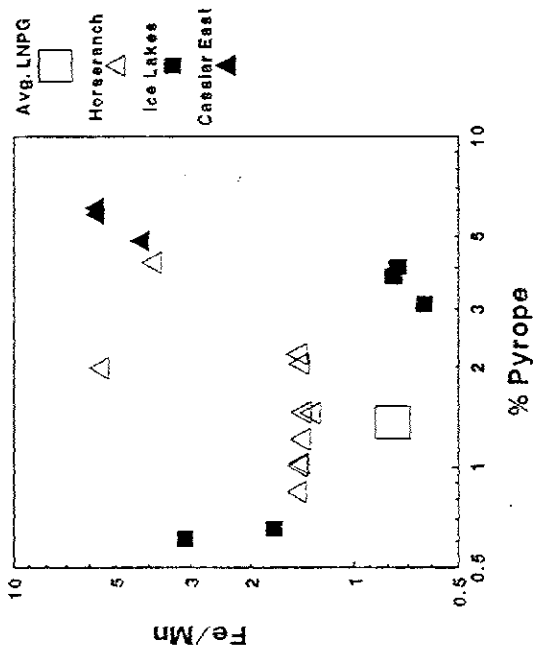


Fig. 3a (left), 3b (right)

Tourmaline

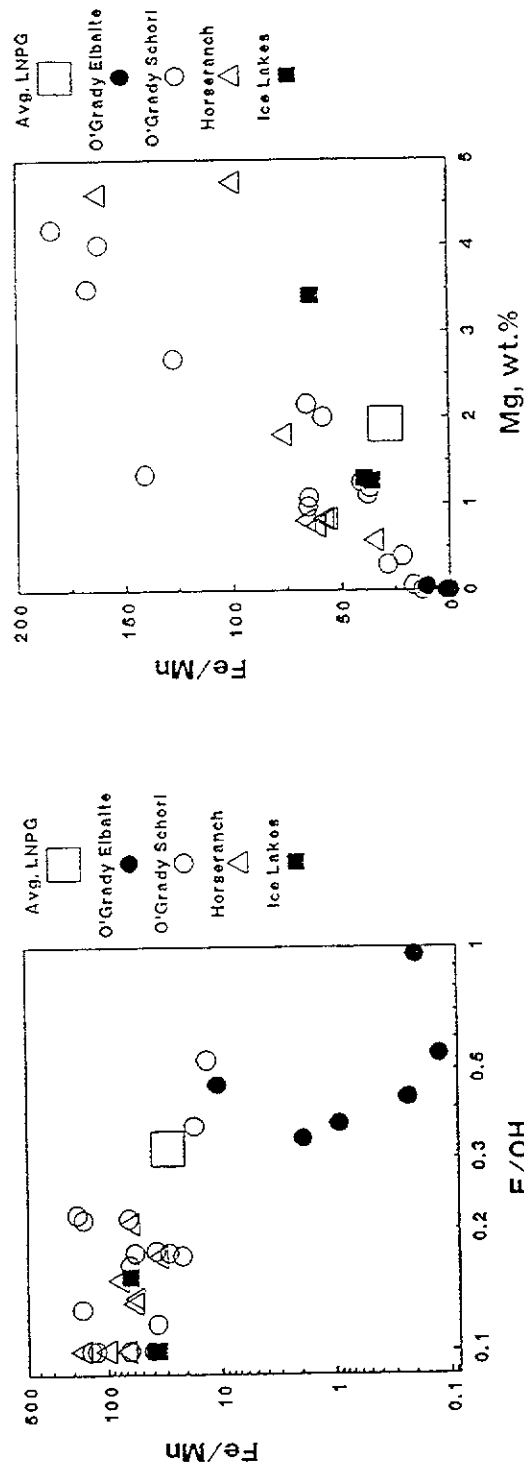


Fig. 4a (top), 4b (bottom)

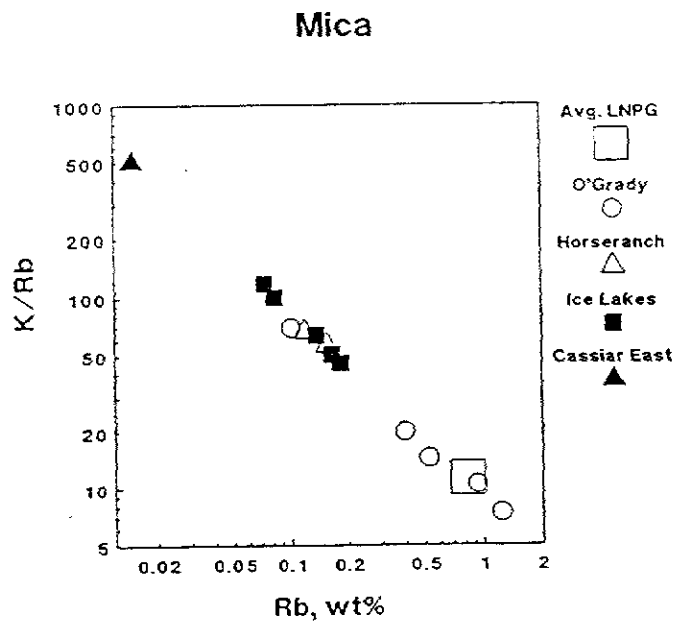
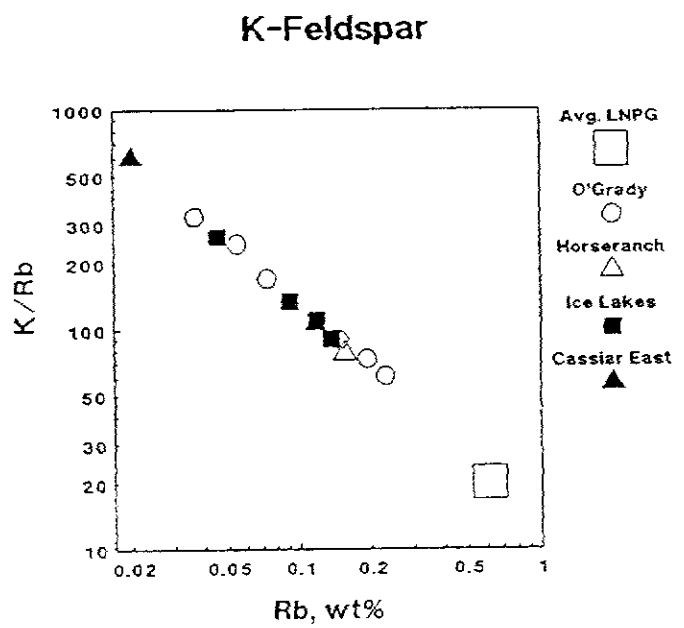


Fig. 5

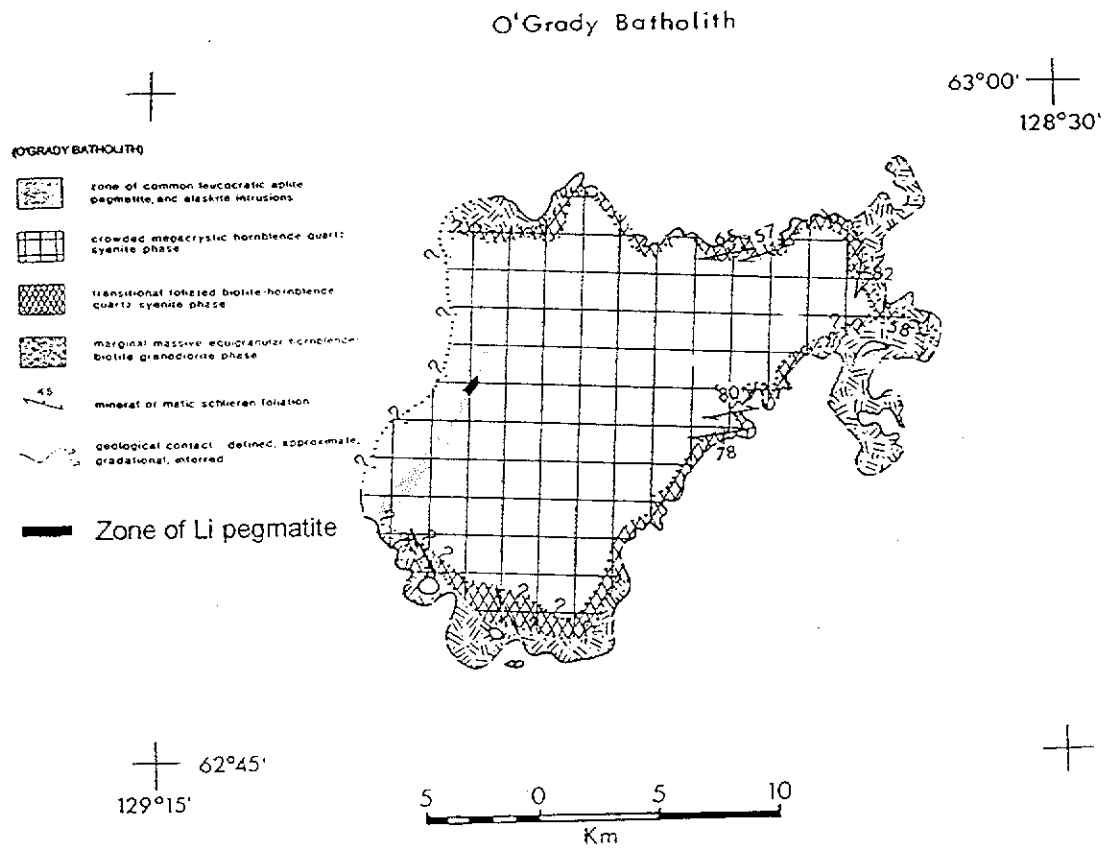


Fig. 6

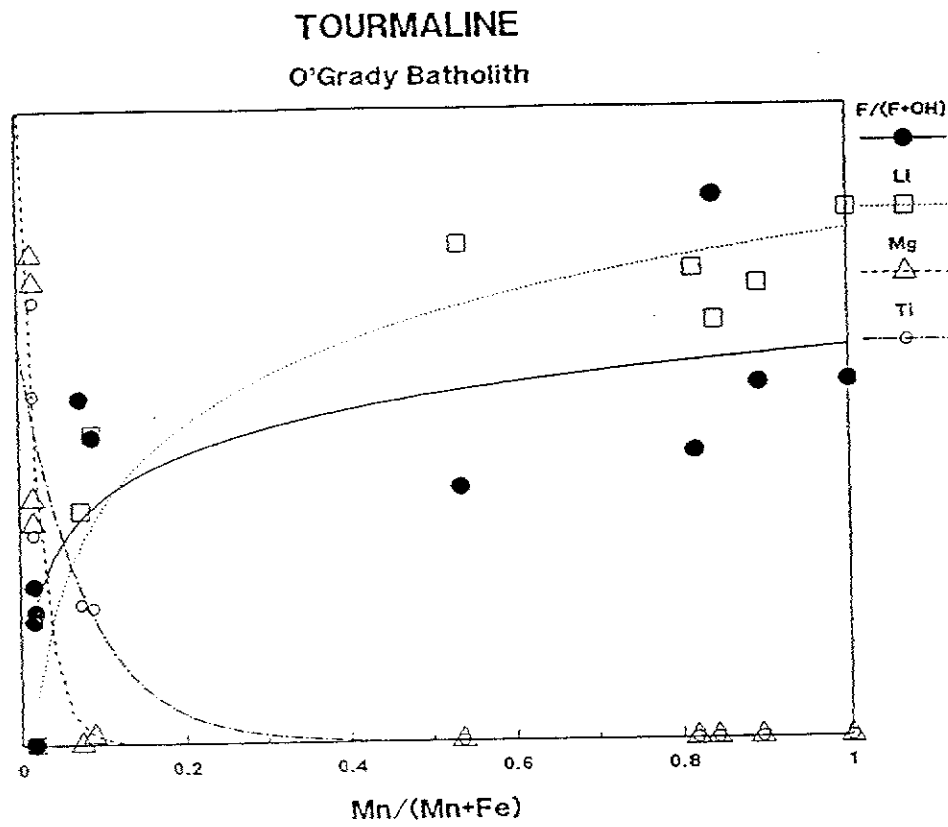
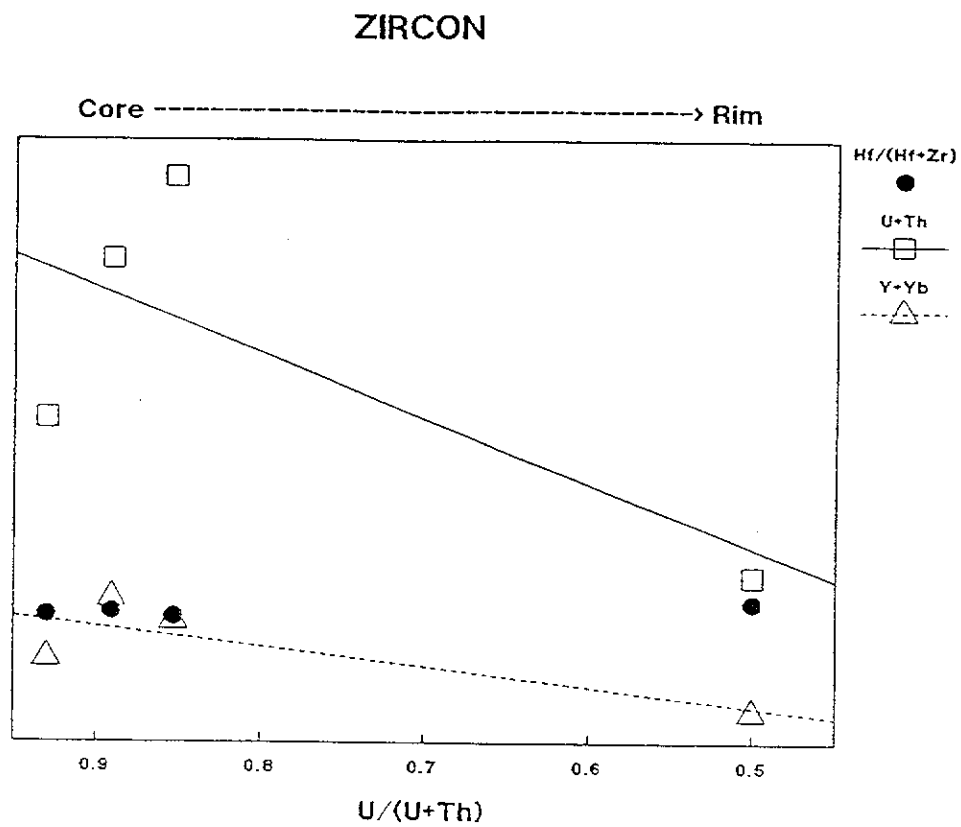


Fig. 7





## APPENDIX 1. MINERAL ANALYSES

### K-feldspar Samples

- KFLN. Average K-feldspar, Little Nahanni Pegmatite Group  
 F1. K-feldspar, Li-pegmatite dyke, cirque 3, O'Grady  
 F2. Cryptoperthite matrix, Li-pegmatite dyke, cirque 3, O'Grady  
 F3. Microperthite matrix, pegmatite dyke, O'Grady  
 F4. Amazonite matrix, pegmatite dyke, cirque 3, cirque 3, O'Grady  
 F5. Microperthite matrix, pegmatite dyke, cirque 3, cirque 3, O'Grady  
 F6. Microperthite matrix, pegmatite dyke, loc. 9, O'Grady  
 F7. Microperthite matrix, pegmatite dyke, loc. 10, O'Grady  
 F8-9. Cryptoperthite, well-zoned dyke between cirques 2,3, Horseranch  
 F10-11. Microperthite matrix, pegmatite dyke, Ice Lakes  
 F12. Microperthite matrix, pegmatite dyke, cirque 2, Ice Lakes  
 F13. Microperthite matrix, pegmatite dyke, cirque 3, Ice Lakes  
 F14-15. Microperthite matrix, pegmatite dyke, "Bimp", Cassiar East

### Plagioclase Lamellae in K-feldspar Samples

- F16. Lamella associated with K-feldspar F3, O'Grady  
 F17. Lamella associated with K-feldspar F4, O'Grady  
 F18. Lamella associated with K-feldspar F5, O'Grady  
 F19. Lamella associated with K-feldspar F6, O'Grady  
 F20. Lamella associated with K-feldspar F10-11, Ice Lakes  
 F21. Lamella associated with K-feldspar F12, Ice Lakes  
 F22. Lamella associated with K-feldspar F13, Ice Lakes  
 F23. Lamella associated with K-feldspar F14-15, "Bimp", Cassiar East

### Plagioclase Samples

- PFLN. Average plagioclase, Little Nahanni Pegmatite Group  
 F24. Albite, Li-pegmatite (associated with Ksp F1), O'Grady  
 F25-26. Albite, pegmatite dyke, O'Grady  
 F27. Oligoclase (var. cleavelandite), pegmatite dyke, loc. 9, O'Grady  
 F28-30. Albite, poorly zoned pegmatite dyke, cirque 3, Horseranch  
 F31-32. Albite, poorly zoned pegmatite dyke, cirque 3, Horseranch  
 F33-34. Albite, pegmatite dyke, Ice Lakes  
 F35-36. Pink graphic oligoclase, pegmatite dyke, "Bimp", Cassiar East

### Mica Samples

- LLN. Average lepidolite/lithian muscovite, Little Nahanni Pegmatite Group  
 M1. Lepidolite, Li-pegmatite dyke, cirque 3, O'Grady  
 M2. Lepidolite, Li-pegmatite dyke, cirque 3, O'Grady  
 M3. Lepidolite, late pocket filling, Li-pegmatite dyke, cirque 3, O'Grady  
 M4. Unknown nappingite-lepidolite-like late green mica, Li-pegmatite dyke, cirque 3, O'Grady  
 M5. Muscovite assoc. with beryl, pegmatite dyke, Horseranch  
 M6-7. Muscovite assoc. with beryl, pegmatite dyke, Ice Lakes  
 M8. Muscovite (plumose), pegmatite dyke, Ice Lakes  
 M9. Muscovite, pegmatite dyke, cirque 2<sup>a</sup>3, Ice Lakes  
 M10. Muscovite (coarse), pegmatite dyke, cirque 2, Ice Lakes  
 M11-12. Muscovite, pegmatite dyke, cirque -2, Cassiar East  
 M13. Biotite, pegmatite dyke, cirque 3, O'Grady  
 M14. Biotite, pegmatite dyke, cirque 3, O'Grady  
 M15. Biotite, pegmatite dyke (wall zone), cirque 2, Ice Lakes

### Tourmaline Samples

- TLLN. Average tourmaline, Little Nahanni Pegmatite Group  
 T1-2. Elbaite, Li-pegmatite dyke, cirque 3 (sample #1, gem red, pink), O'Grady  
 T3. Lithian schorl, Li-pegmatite dyke, cirque 3 (sample #2, blue-black core), O'Grady  
 T4. Elbaite, Li-pegmatite dyke, cirque 3 (sample #2, gem red rim), O'Grady  
 T5. Ferroan elbaite, Li-pegmatite dyke, cirque 3 (sample #3, green-black core), O'Grady  
 T6-7. Elbaite, Li-pegmatite dyke, cirque 3 (sample #4, late, pink gem, 6=core, 7=rim), O'Grady  
 T8. Elbaite, Li-pegmatite dyke, cirque 3 (sample #7, colourless), O'Grady  
 T9. Elbaite, Li-pegmatite dyke, cirque 3 (assoc. nappingite), O'Grady  
 T10. Schorl, pegmatite dyke, O'Grady  
 T11-13. Schorl, pegmatite dyke, O'Grady  
 T14-17. Schorl, pegmatite dyke, loc. 1, cirque 2, O'Grady  
 T18. Schorl, pegmatite dyke, loc. 7, O'Grady  
 T19-20. Schorl, pegmatite dyke, loc. 9, O'Grady  
 T21-22. Schorl, pegmatite dyke, loc. 10, O'Grady  
 T23-24. Feruvite-schorl, pegmatoid patch in aplite dyke (OG-1), cirque 1, O'Grady  
 T25. Schorl, apilite dyke, cirque 2, O'Grady  
 T26-27. Schorl, pegmatite dyke, cirque 3, Horseranch  
 T28-29. Schorl, pegmatite dyke, cirque 3, Horseranch  
 T30-31. Schorl, pegmatite dyke, cirque 3, Horseranch  
 T32. Schorl, pegmatite dyke, cirque -1, Horseranch  
 T33. Schorl, pegmatite dyke, cirque -1, Horseranch  
 T34-36. Dravite-schorl, pegmatite dyke, cirque 2, Ice Lakes

Axinite Samples

- AX1. Ferroaxinite, pegmatite dyke, O'Grady  
 AX2-3. Ferroaxinite, patchy zoned, pegmatite dyke, loc. 9, O'Grady  
 AX4-5. Ferroaxinite, pegmatite dyke, pegmatite dyke, loc. 9, O'Grady

Danburite Samples

- D1. Danburite, pocket, LI-pegmatite dyke, cirque 3, O'Grady

Hamborgite Samples

- H1. Hamborgite, pocket, LI-pegmatite dyke, cirque 3, O'Grady (inclusion in elbaite)

Beryl Samples

- BLN. Average beryl, Little Nahanni Pegmatite Group  
 B1-2. Beryl crystal, pegmatite dyke, cirque 3, Horseranch  
 B3-4. Beryl crystal, pegmatite dyke, cirque 3, Horseranch  
 B5-6. Beryl crystal, pegmatite dyke, cirque 3, Horseranch  
 B7-10. Beryl crystal, well-zoned pegmatite dyke, cirque 2<sup>nd</sup>3, Horseranch  
 (7,8=rim, 9,10=core)  
 B11-14. Beryl crystal, pegmatite dyke, Ice Lakes (11,12=core, 13,14=rim)  
 B15-18. Beryl crystal, pegmatite dyke, Ice Lakes (15,16=core, 17,18=rim)  
 B19. Beryl crystal, pegmatite dyke, cirque 2<sup>nd</sup>3, Ice Lakes

Garnet Samples

- GLN. Average garnet, Little Nahanni Pegmatite Group  
 G1-2. Mn-rich almandine, pegmatite dyke, cirque 3, Horseranch (1=rim, 2=core)  
 G3-4. Mn-rich almandine, pegmatite dyke, cirque 3, Horseranch (3=rim, 4=core)  
 G5-7. Mn-rich almandine, pegmatite dyke, cirque 3, Horseranch  
 (5=core, 6=interm., 7=rim)  
 G8. Mn-rich almandine, pegmatite dyke, cirque 1, Horseranch  
 G9. Almandine, pegmatite dyke, cirque 4, Horseranch  
 G10. Mn-rich almandine, pegmatite dyke, cirque 3, Horseranch  
 G11-12. Spessartine, pegmatite dyke, cirque 3, Ice Lakes (11=core, 12=rim)  
 G13. Spessartine, pegmatite dyke, Ice Lakes  
 G14-15. Spessartine, pegmatite dyke, cirque 2, Ice Lakes  
 G16-18. Almandine, pegmatite dyke, "Bimp", Cassiar East

Titanite Samples

- TT1. Titanite, pegmatite dyke, O'Grady  
 TT2. Titanite, pegmatite dyke, O'Grady  
 TT3-4. Titanite, oscillatory zoned, pegmatite dyke, loc. 1, cirque 2, O'Grady  
 TT5. Titanite assoc. ilmenite, pegmatite dyke, cirque 3, O'Grady  
 TT6. Titanite assoc. schorl, pegmatite dyke, loc. 9, O'Grady  
 TT7-8. Titanite assoc. magnetite and pseudorutile, pegmatite dyke, loc. 9, O'Grady  
 TT9. Titanite, pegmatite dyke, loc. 9, O'Grady

Allanite Samples

- A1: Allanite-(Ce), pegmatite dyke near LI pegmatites, cirque 3, O'Grady  
 A2: Allanite-(La), pegmatite dyke, cirque 3, O'Grady  
 A3: Allanite-(Ce), pegmatite dyke, cirque 3, O'Grady  
 A4-5: Allanite-(Ce), pegmatite dyke, loc. 9, O'Grady  
 A6: Allanite-(Ce), pegmatite dyke, loc. 9, O'Grady  
 A7: Allanite-(Ce), pegmatite dyke, loc. 10, O'Grady

Zircon Samples

- Z1-4. Zircon grain, pegmatite dyke, O'Grady (1-3=core, 4=rim)

Columbite-Tantalite Samples

- CT1-2. Ferrocolumbite / ixiolite, pegmatite dyke, cirque 2, Ice Lakes  
 CT3. Ferrocolumbite, pegmatite dyke, cirque 3, Ice Lakes

Rutile Samples

- RT 1. Tantalum-niobian rutile, pegmatite dyke, Ice Lakes (intergrown with columbite CT1,2)

Pseudorutile Samples

- PR1. Pseudorutile, replaces ilmenite IL1, pegmatite dyke, loc. 9, O'Grady

Ilmenite Samples

- IL1. Ilmenite, pegmatite dyke, loc. 9, O'Grady
- IL2. Ilmenite, pegmatite dyke, O'Grady
- IL3-4. Ilmenite, pegmatite dyke, O'Grady (3=core, 4=rim)
- IL5. Ilmenite lamella in magnetite sample MT2, O'Grady

Spinel Samples

- MT1. Magnetite, pegmatite dyke, O'Grady
- MT2. Magnetite, pegmatite dyke, O'Grady
- GN1. Garnet inclusion in beryl sample B3-4, pegmatite dyke, Horseranch

Scheelite Samples

- SC1. Scheelite associated with magnetite MT1, O'Grady

Apatite Samples

- APLN. Average apatite, Little Nahanni Pegmatite Group
- AP1-2: Fluorapatite, pegmatite dyke, cirque 3E, Horseranch
- AP3-4: Fluorapatite, pegmatite dyke, cirque 3E, Horseranch
- AP5-6: Fluorapatite, pegmatite dyke, cirque 3E, Horseranch
- AP7-8: Fluorapatite, pegmatite dyke, "Bimp", Cassiar East

Miscellaneous Phosphate Minerals

- P1: Wagnerite (primary), pegmatite dyke, Ice Lakes
- P2: Triplidite (replaces spessartine), pegmatite dyke, Ice Lakes
- P3: Monazite-(Ce) inclusion in Wagnerite P1, Ice Lakes

NOTES FOR TABLES

Asterisks denote components calculated by stoichiometry. "0.00": not detected, "----": not sought.



TABLE 1. (cont.)

	F21	F22	F23	PFLN	F24	F25	F26	F27	F28	F29	F30	F31	F32	F33	F34	F35	F36
SiO2	88.10	67.98	69.01	68.80	69.04	65.16	67.66	60.66	68.11	67.74	67.51	68.22	68.59	66.67	66.44	63.35	63.40
P2O5	0.44	0.33	0.00	0.20	0.00	0.00	0.00	0.00	0.00	0.00	0.16	0.18	0.12	0.35	0.41	0.00	0.00
Al2O3	20.17	19.67	19.62	18.90	19.70	21.19	19.90	24.36	20.25	20.26	20.12	20.47	19.87	20.56	20.72	23.50	23.57
Fe2O3	0.06	0.07	0.00	0.00	0.00	0.00	0.00	0.22	0.00	0.06	0.00	0.00	0.00	0.00	0.00	0.00	0.00
MnO	0.00	0.00	0.00	0.00	0.00	0.00	0.00	0.00	0.00	0.00	0.00	0.00	0.00	0.00	0.00	0.00	0.00
CaO	0.42	0.11	0.30	0.07	0.00	0.67	0.38	6.00	0.69	0.97	0.69	0.80	0.35	0.47	0.55	4.62	4.58
SrO	0.04	0.05	0.07	0.04	0.00	0.05	0.00	0.00	0.06	0.04	0.05	0.06	0.05	0.04	0.04	0.15	0.16
BaO	0.00	0.00	0.00	0.00	0.00	0.00	0.00	0.00	0.00	0.00	0.00	0.00	0.00	0.00	0.00	0.00	0.00
Na2O	11.36	11.56	11.42	11.10	11.84	10.92	11.52	7.45	11.48	11.14	11.15	11.26	11.49	11.40	11.26	8.95	9.01
K2O	0.27	0.18	0.18	0.13	0.05	0.07	0.00	0.60	0.14	0.22	0.22	0.21	0.18	0.11	0.19	0.27	0.10
Rb2O	0.00	0.00	0.00	0.00	0.00	0.00	0.00	0.00	0.00	0.00	0.00	0.00	0.00	0.00	0.00	0.00	0.00
Cs2O	0.00	0.00	0.00	0.00	0.00	0.00	0.00	0.00	0.00	0.00	0.00	0.00	0.00	0.00	0.00	0.00	0.00
	100.86	99.95	100.60	99.24	100.63	98.26	99.46	99.29	100.73	100.43	99.90	101.20	100.65	99.59	99.61	100.84	100.82

	F21	F22	F23	F24	F25	F26	F27	F28	F29	F30	F31	F32	F33	F34	F35	F36
Si	11.810	11.889	11.985	12.072	11.980	11.624	11.892	10.864	11.844	11.822	11.828	11.803	11.915	11.718	11.680	11.130
P	0.065	0.049	0.000	0.030	0.000	0.000	0.000	0.000	0.000	0.000	0.024	0.026	0.018	0.052	0.061	0.000
Al	4.123	4.054	4.016	3.908	4.028	4.456	4.120	5.142	4.150	4.167	4.155	4.174	4.068	4.257	4.293	4.866
Fe3+	0.008	0.009	0.000	0.000	0.000	0.000	0.000	0.030	0.000	0.008	0.000	0.000	0.000	0.000	0.000	0.000
Mn	0.000	0.000	0.000	0.000	0.000	0.000	0.000	0.000	0.000	0.000	0.000	0.000	0.000	0.000	0.000	0.000
Ca	0.078	0.021	0.056	0.013	0.000	0.168	0.072	1.151	0.129	0.181	0.130	0.148	0.065	0.089	0.104	0.870
Sr	0.004	0.005	0.007	0.004	0.000	0.004	0.000	0.000	0.006	0.004	0.005	0.006	0.005	0.004	0.004	0.015
Ba	0.000	0.000	0.000	0.000	0.000	0.000	0.000	0.000	0.000	0.000	0.000	0.000	0.000	0.000	0.000	0.000
Na	3.820	3.920	3.845	3.776	3.984	3.776	3.924	2.587	3.871	3.769	3.788	3.777	3.870	3.885	3.838	3.049
K	0.060	0.040	0.040	0.029	0.012	0.016	0.000	0.137	0.031	0.049	0.049	0.046	0.040	0.025	0.043	0.061
Rb	0.000	0.000	0.000	0.000	0.000	0.000	0.000	0.000	0.000	0.000	0.000	0.000	0.000	0.000	0.000	0.000
Cs	0.000	0.000	0.000	0.000	0.000	0.000	0.000	0.000	0.000	0.000	0.000	0.000	0.000	0.000	0.000	0.000
	19.967	19.986	19.949	19.832	20.004	20.044	20.008	19.912	20.031	20.000	19.978	19.982	19.980	20.030	20.022	19.991

	32	32	32	32	32	32	32	32	32	32	32	32	32	32	32	32
O	2	1	1	1	0	0	0	4	1	1	1	1	1	1	1	2
%O1	97	98	98	99	100	95	98	67	96	94	95	95	97	97	96	77
%Ab	2	1	1	0	0	4	2	30	3	5	4	4	2	2	3	22
%An																
K/Rb																
K/Cs																
P (ppm)	1920	1430	170	870	<120	<120	<120	---	<120	<120	680	790	530	1780	<120	<120
Sr (ppm)	340	430	570	350	<200	400	<200	---	470	350	400	510	380	350	310	1280
Ba (ppm)	<250	<250	<250	<250	<250	<250	<250	<250	<250	<250	<250	<250	<250	<250	<250	<250

Formula Contents per 32 (O)

TABLE 2. CHEMICAL COMPOSITION OF MICA

	LLN	M1	M2	M3	M4*	M5	M6	M7	M8	M9	M10	M11	M12	M13	M14	M15
SiO2	49.03	60.11	58.31	56.72	47.47	45.67	45.53	45.80	45.14	45.01	43.96	45.98	46.38	35.72	37.96	35.27
TiO2	0.00	---	---	---	---	---	0.18	0.51	0.18	0.25	0.30	---	---	4.69	3.67	3.04
Al2O3	27.74	15.67	16.66	18.70	14.36	36.60	32.65	33.63	36.20	34.19	33.64	35.00	34.87	13.84	14.19	18.44
MgO	---	0.00	0.00	0.00	0.00	0.00	0.95	0.83	0.58	0.66	1.01	0.92	0.95	10.65	6.60	8.02
MnO	0.24	0.08	0.00	0.00	0.00	0.00	0.05	0.00	0.06	0.00	0.05	0.00	0.00	0.28	0.86	0.69
FeO	0.00	0.08	0.00	0.41	2.32	1.36	4.57	4.00	2.76	3.46	3.84	1.92	1.86	19.27	22.19	19.96
CaO	0.00	0.00	0.08	0.06	0.14	0.06	0.05	0.04	0.00	0.00	0.00	0.05	0.00	0.75	0.00	0.00
SrO	0.03	0.00	0.15	0.06	0.00	0.07	0.06	0.05	0.07	0.07	0.06	0.07	0.07	0.07	0.05	0.07
BaO	0.00	0.00	0.00	0.00	0.00	0.00	0.00	0.00	0.00	0.00	0.00	0.30	0.31	0.00	0.00	0.00
Li2O*	4.73	6.81	6.86	6.24	4.77	---	---	---	---	---	---	---	---	---	---	---
Na2O	0.29	0.00	0.16	0.05	0.00	0.68	0.27	0.47	0.77	0.78	0.74	0.65	0.62	0.00	0.00	0.12
K2O	11.10	11.61	10.86	9.00	1.12	10.54	10.47	10.00	10.36	9.98	9.88	10.51	10.43	8.39	9.40	9.51
Rb2O	0.90	1.01	1.34	0.57	0.17	0.17	0.15	0.18	0.08	0.20	0.09	0.00	0.00	0.11	0.43	0.13
Cs2O	0.04	0.39	1.14	1.25	17.02	0.00	0.00	0.00	0.00	0.00	0.00	0.00	0.00	0.00	0.28	0.00
H2O*	1.63	0.52	0.50	0.76	0.85	4.51	4.40	4.45	4.24	4.23	4.15	4.48	4.49	3.24	2.98	3.55
F	6.02	8.66	8.59	7.93	6.07	0.00	0.00	0.00	0.55	0.39	0.43	0.00	0.00	1.29	1.88	0.75
O=F	<u>-2.53</u>	<u>-3.65</u>	<u>-3.62</u>	<u>-3.34</u>	<u>-2.56</u>	<u>0.00</u>	<u>0.00</u>	<u>0.00</u>	<u>-0.23</u>	<u>-0.16</u>	<u>-0.18</u>	<u>0.00</u>	<u>0.00</u>	<u>-0.54</u>	<u>-0.79</u>	<u>-0.32</u>
	99.22	101.29	101.03	98.41	91.98	100.15	99.33	99.96	100.76	99.06	97.97	99.88	100.03	97.76	99.70	99.23

Formula Contents per 24 anions

Si	6.557	7.799	7.645	7.529	7.637	6.073	6.206	6.168	6.012	6.115	6.056	6.155	6.190	5.557	5.886	5.418
Ti	0.000	---	---	---	---	---	0.018	0.052	0.018	0.026	0.031	---	---	0.549	0.428	0.351
Al	4.372	2.396	2.574	2.926	2.723	5.736	5.245	5.338	5.682	5.474	5.462	5.521	5.485	2.537	2.593	3.339
Mg	---	0.000	0.000	0.000	0.050	0.097	0.193	0.167	0.115	0.134	0.207	0.184	0.189	2.470	1.526	1.837
Mn	0.027	0.009	0.000	0.000	0.000	0.006	0.000	0.000	0.007	0.000	0.006	0.000	0.000	0.037	0.113	0.090
Fe2+	0.000	0.009	0.000	0.046	0.312	0.151	0.521	0.450	0.307	0.393	0.442	0.215	0.208	2.507	2.878	2.564
Ca	0.000	0.000	0.011	0.009	0.024	0.009	0.007	0.006	0.000	0.000	0.000	0.007	0.007	0.125	0.000	0.000
Sr	0.002	0.000	0.011	0.005	0.004	0.005	0.005	0.004	0.005	0.006	0.005	0.005	0.005	0.006	0.004	0.006
Ba	0.000	0.000	0.000	0.000	0.000	0.000	0.000	0.000	0.000	0.000	0.000	0.016	0.016	0.000	0.000	0.000
Li	2.546	3.553	3.617	3.330	3.086	---	---	---	---	---	---	---	---	---	---	---
Na	0.075	0.000	0.041	0.013	0.000	0.175	0.071	0.123	0.199	0.205	0.198	0.169	0.160	0.000	0.000	0.036
K	1.894	1.922	1.817	1.524	0.230	1.788	1.821	1.718	1.760	1.730	1.737	1.795	1.776	1.665	1.860	1.864
Rb	0.077	0.084	0.113	0.049	0.018	0.015	0.013	0.016	0.007	0.017	0.008	0.000	0.000	0.011	0.043	0.013
Cs	0.002	0.022	0.064	0.071	1.168	0.000	0.000	0.000	0.000	0.000	0.000	0.000	0.000	0.000	0.019	0.000
	15.552	15.794	15.893	15.502	15.252	14.049	14.106	14.042	14.112	14.100	14.152	14.067	14.036	15.464	15.350	15.518
OH	1.454	0.446	0.438	0.670	0.911	4.000	4.000	4.000	3.768	3.832	3.813	4.000	4.000	3.365	3.078	3.636
F	2.546	3.554	3.562	3.330	3.089	0.000	0.000	0.000	0.232	0.168	0.187	0.000	0.000	0.635	0.922	0.364
O	20.000	20.000	20.000	20.000	20.000	20.000	20.000	20.000	20.000	20.000	20.000	20.000	20.000	20.000	20.000	20.000
K/Rb	11	10	7	14	6	56	63	50	118	45	100	>500	>500	69	20	66
K/Cs	244	26	8	6	0.1	>300	>300	>300	>300	>300	>300	>300	>300	>300	30	>275
Sr (ppm)	250	<200	1280	530	275	630	520	460	590	610	530	600	630	580	460	620
Ba (ppm)	<250	<250	<250	<250	<250	<250	<250	<250	<250	<250	<250	2700	2758	<250	<250	<250

\* Li calc. assuming F=Li (atomic) \*\* M4 was too fine-grained for a high-quality analysis, hence low analytical sum

TABLE 3. CHEMICAL COMPOSITION OF TOURMALINE AND OTHER BORON-BEARING MINERALS

	TLN	T1	T2	T3	T4	T5	T6	T7	T8	T9	T10	T11	T12	T13	T14	T15	T16	T17	T18	T19	T20	T21
SiO <sub>2</sub>	34.33	36.81	36.86	34.83	37.24	35.83	36.98	35.86	37.72	37.36	33.56	33.55	33.72	33.63	33.94	34.60	33.82	34.01	35.04	34.23	33.71	34.88
TiO <sub>2</sub>	0.97	0.00	0.00	0.61	0.00	0.60	0.00	0.00	0.00	0.00	1.80	1.43	1.44	0.87	2.34	2.64	1.06	1.27	0.81	1.47	0.80	0.21
B <sub>2</sub> O <sub>3</sub> *	10.17	11.00	11.04	10.29	10.97	10.51	10.92	10.66	11.24	11.13	9.65	9.69	9.74	9.78	9.85	10.02	9.66	9.72	10.10	9.84	9.69	9.99
Al <sub>2</sub> O <sub>3</sub>	31.81	41.28	42.04	33.71	39.34	35.05	40.00	38.00	43.13	42.70	22.43	24.45	24.64	25.69	26.45	28.32	23.55	24.30	32.00	22.74	26.64	26.96
V <sub>2</sub> O <sub>3</sub>	0.04	0.00	0.00	0.00	0.00	0.00	0.00	0.00	0.00	0.00	0.09	0.00	0.08	0.00	0.10	0.08	0.00	0.06	0.00	0.24	0.00	0.21
BeO*	---	---	---	---	---	---	---	---	---	---	---	---	---	---	---	---	---	---	---	---	---	---
MgO	3.17	0.00	0.00	0.00	0.00	0.07	0.00	0.00	0.00	0.00	3.32	1.78	1.61	3.57	0.50	0.66	2.08	1.97	0.09	6.67	0.20	5.82
MnO	0.37	0.21	0.11	0.86	3.28	0.81	1.85	4.19	0.08	0.00	0.36	0.33	0.33	0.27	0.68	0.73	0.54	0.56	0.77	0.10	0.00	0.08
FeO	10.67	0.00	0.10	11.06	0.40	8.53	0.42	0.81	0.15	0.23	20.84	21.23	21.39	17.64	19.31	15.81	21.80	20.45	12.86	16.15	21.46	13.33
ZnO	---	---	---	---	---	---	---	---	---	---	---	---	---	---	---	---	---	---	---	---	---	---
CaO	0.55	1.96	1.16	0.34	1.08	0.34	0.98	0.74	0.41	0.08	1.75	1.23	1.25	1.46	0.75	0.69	1.70	1.42	0.36	2.28	0.60	1.05
Li <sub>2</sub> O*	0.11	2.30	2.17	0.95	1.97	1.29	2.03	1.76	2.05	2.03	0.00	0.00	0.00	0.00	---	---	---	---	---	---	---	---
Na <sub>2</sub> O	2.20	1.56	1.93	2.71	2.39	2.83	2.23	2.83	2.02	2.38	1.86	2.13	2.11	2.01	2.31	2.39	1.76	1.99	2.62	1.54	2.09	2.22
K <sub>2</sub> O	0.04	0.00	0.00	0.00	0.00	0.00	0.00	0.00	0.00	0.00	0.07	0.04	0.06	0.05	0.06	0.00	0.05	0.06	0.00	0.05	0.04	0.05
H <sub>2</sub> O	3.07	3.04	3.27	2.87	3.04	3.01	3.16	2.57	3.37	3.68	3.09	3.12	3.36	3.08	3.15	3.21	3.33	3.19	3.00	3.10	3.34	3.26
F	0.92	1.58	1.13	1.43	1.57	1.30	1.27	2.33	1.07	0.34	0.51	0.48	0.00	0.62	0.52	0.52	0.00	0.35	1.02	0.62	0.00	0.39
O=F	-0.39	-0.67	-0.48	-0.60	-0.66	-0.55	-0.53	-0.98	-0.45	-0.14	-0.21	-0.20	0.00	-0.26	-0.22	-0.22	0.00	-0.15	-0.43	-0.26	0.00	-0.16
	98.03	99.07	99.32	99.06	100.62	99.62	99.31	98.77	100.79	99.79	99.12	99.26	99.73	98.41	99.74	99.45	99.35	99.20	98.24	98.77	98.57	98.09
Si	5.868	5.818	5.799	5.883	5.902	5.925	5.888	5.849	5.834	5.835	6.046	6.019	6.019	5.978	5.990	6.003	6.083	6.084	6.031	6.048	6.043	6.035
Ti	0.125	0.000	0.000	0.077	0.000	0.075	0.000	0.000	0.000	0.000	0.244	0.193	0.193	0.116	0.311	0.344	0.143	0.171	0.105	0.195	0.108	0.027
B	3.000	3.000	3.000	3.000	3.000	3.000	3.000	3.000	3.000	3.000	3.000	3.000	3.000	3.000	3.000	3.000	3.000	3.000	3.000	3.000	3.000	3.000
Al	6.408	7.689	7.798	6.444	7.349	6.831	7.506	7.305	7.862	7.860	4.762	5.169	5.184	5.382	5.501	4.992	4.992	5.123	6.492	4.735	5.629	5.529
V	0.005	0.000	0.000	0.000	0.000	0.000	0.000	0.000	0.000	0.000	0.013	0.000	0.011	0.000	0.014	0.011	0.000	0.009	0.000	0.034	0.000	0.029
Be	---	---	---	---	---	---	---	---	---	---	---	---	---	---	---	---	---	---	---	---	---	---
Mg	0.808	0.000	0.000	0.000	0.000	0.017	0.000	0.000	0.000	0.000	0.892	0.476	0.428	0.946	0.132	0.171	0.558	0.525	0.023	1.757	0.053	1.510
Mn	0.054	0.028	0.015	0.123	0.440	0.113	0.249	0.579	0.010	0.000	0.055	0.050	0.050	0.041	0.102	0.107	0.082	0.085	0.112	0.015	0.000	0.012
Fe <sup>2+</sup>	1.525	0.000	0.013	1.562	0.053	1.180	0.056	0.110	0.019	0.030	3.140	3.185	3.193	2.622	2.650	2.294	3.279	3.059	1.851	2.386	3.218	1.940
Zn	---	---	---	---	---	---	---	---	---	---	---	---	---	---	---	---	---	---	---	---	---	---
Ca	0.101	0.332	0.196	0.062	0.183	0.080	0.167	0.129	0.068	0.013	0.338	0.236	0.239	0.278	0.142	0.128	0.328	0.272	0.066	0.432	0.115	0.196
Li	0.076	1.462	1.373	0.645	1.256	0.858	1.300	1.155	1.275	1.275	0.000	0.000	0.000	0.000	0.000	0.000	0.000	0.000	0.000	0.000	0.000	0.000
Na	0.729	0.478	0.589	0.887	0.734	0.907	0.688	0.895	0.606	0.721	0.650	0.741	0.730	0.693	0.790	0.804	0.614	0.690	0.874	0.528	0.726	0.749
K	0.009	0.000	0.000	0.000	0.000	0.000	0.000	0.000	0.000	0.000	0.016	0.009	0.014	0.011	0.014	0.011	0.011	0.014	0.000	0.011	0.009	0.011
	18.707	18.807	18.783	18.950	18.917	18.966	18.854	19.022	18.675	18.734	19.156	19.078	19.061	19.067	18.846	18.653	19.090	19.032	18.554	19.141	18.901	19.038
OH	3.503	3.210	3.438	3.236	3.213	3.320	3.361	2.798	3.477	3.832	3.709	3.728	4.000	3.651	3.710	3.715	4.000	3.802	3.445	3.654	4.000	3.785
F	0.497	0.790	0.562	0.784	0.787	0.680	0.639	1.202	0.523	0.168	0.291	0.272	0.000	0.349	0.290	0.285	0.000	0.198	0.555	0.346	0.000	0.215
O	27.000	27.000	27.000	27.000	27.000	27.000	27.000	27.000	27.000	27.000	27.000	27.000	27.000	27.000	27.000	27.000	27.000	27.000	27.000	27.000	27.000	27.000
Fe/Mn	29	0	1	13	0	11	0	0	2	>6	58	65	65	66	29	22	41	37	17	162	>550	167
F/OH	0.32	0.55	0.37	0.53	0.55	0.46	0.43	0.96	0.34	0.10	0.17	0.16	<0.10	0.21	0.17	0.17	<0.10	0.12	0.36	0.21	<0.10	0.13

Tourmaline formulae on a basis of 31 anions, axinite on 16 anions, danburite on 8 (O), hambergite on 4 anions.

Formula Contents

TABLE 3. (cont.)

	T22	T23	T24	T25	T26	T27	T28	T29	T30	T31	T32	T33	T34	T35	T36	AX1	AX2	AX3	AX4	AX5	D1	H1
SiO2	34.45	34.27	34.14	32.78	34.91	35.18	35.15	34.97	34.57	34.70	35.36	35.96	34.24	35.15	34.10	42.21	41.50	41.65	41.58	41.82	49.90	---
TiO2	0.40	0.86	0.15	1.91	0.10	0.15	0.12	0.14	0.27	0.13	0.52	0.68	0.39	0.42	0.40	0.00	0.00	0.15	0.00	0.00	---	---
B2O3*	9.77	9.91	9.84	9.56	10.40	10.38	10.36	10.34	10.24	10.28	10.46	10.51	10.22	10.35	10.17	6.11	6.04	6.01	6.01	6.03	28.94	36.95
Al2O3	24.46	24.24	27.34	23.72	34.42	33.92	33.77	33.90	33.92	33.67	33.42	32.78	32.82	31.53	32.66	17.62	17.36	16.51	17.21	17.17	---	---
V2O3	0.25	0.08	0.00	0.06	0.00	0.00	0.00	0.00	0.00	0.00	0.00	0.05	0.00	0.00	0.00	0.00	---	---	---	---	---	
BeO*	---	---	---	---	---	---	---	---	---	---	---	---	---	---	---	---	---	---	---	---	---	53.10
MgO	4.46	6.96	2.23	1.84	1.37	1.23	1.37	1.34	0.58	1.80	4.74	4.61	2.15	5.66	2.10	1.29	1.25	0.87	0.90	0.90	0.00	---
MnO	0.14	0.08	0.13	0.57	0.24	0.23	0.25	0.21	0.41	0.17	0.09	0.06	0.34	0.15	0.37	1.66	3.93	4.04	3.55	3.98	0.00	---
FeO	17.73	14.64	18.26	21.26	13.54	13.82	13.64	13.62	13.66	12.83	8.87	9.66	13.21	9.46	13.15	9.30	7.38	8.42	8.05	7.78	0.00	---
ZnO	0.00	0.00	0.00	0.00	0.29	0.28	0.23	0.21	0.35	0.28	0.00	0.00	0.31	0.18	0.33	---	---	---	---	---	---	---
CaO	0.98	2.65	1.00	1.27	0.11	0.10	0.10	0.09	0.08	0.11	0.30	0.26	0.07	0.18	0.08	19.50	19.45	19.32	19.20	19.09	23.40	---
Li2O*	---	---	---	---	---	---	---	---	---	---	---	---	---	---	---	---	---	---	---	---	---	---
Na2O	2.14	1.34	2.07	2.02	1.92	1.94	1.90	1.94	1.89	2.03	2.02	1.97	2.11	2.41	2.13	0.00	0.00	0.00	0.00	0.00	0.00	---
K2O	0.04	0.06	0.04	0.06	0.05	0.00	0.05	0.00	0.00	0.00	0.04	0.00	0.04	0.00	0.05	0.00	0.00	0.00	0.00	0.00	0.00	---
H2O*	3.37	3.11	3.39	3.06	3.39	3.28	3.37	3.57	3.28	3.33	3.61	3.63	3.52	3.34	3.51	1.58	1.56	1.55	1.56	1.56	---	7.85
F	0.00	0.64	0.00	0.51	0.42	0.64	0.43	0.00	0.53	0.47	0.00	0.00	0.00	0.48	0.00	0.00	0.00	0.00	0.00	0.00	0.00	3.61
O=F	0.00	-0.27	0.00	-0.21	-0.18	-0.27	-0.18	0.00	-0.22	-0.20	0.00	0.00	0.00	-0.20	0.00	0.00	0.00	0.00	0.00	0.00	0.00	1.52
	98.19	98.57	98.59	98.41	100.98	100.88	100.55	100.33	99.56	99.60	99.43	100.17	99.42	99.13	99.05	99.27	98.47	98.52	98.06	98.33	102.2	99.99

Formula Contents

Si	6.125	6.012	6.033	5.958	5.834	5.890	5.899	5.877	5.869	5.864	5.875	5.947	5.825	5.905	5.826	4.004	3.982	4.017	4.008	4.019	1.998	---
Ti	0.053	0.113	0.020	0.261	0.013	0.019	0.015	0.018	0.034	0.017	0.065	0.085	0.050	0.053	0.051	0.000	0.000	0.011	0.000	0.000	---	---
B	3.000	3.000	3.000	3.000	3.000	3.000	3.000	3.000	3.000	3.000	3.000	3.000	3.000	3.000	3.000	1.000	1.000	1.000	1.000	1.000	2.000	1.000
Al	5.126	5.012	5.694	5.081	6.779	6.693	6.679	6.715	6.786	6.706	6.545	6.389	6.581	6.243	6.576	1.970	1.963	1.876	1.955	1.945	---	---
V	0.036	0.011	0.000	0.009	0.000	0.000	0.000	0.000	0.000	0.000	0.000	0.007	0.000	0.000	0.000	0.000	---	---	---	---	---	2.000
Be	1.182	1.820	0.587	0.499	0.341	0.307	0.343	0.336	0.147	0.453	1.174	1.137	0.545	1.422	0.535	0.182	0.179	0.125	0.129	0.129	0.000	---
Mg	0.021	0.012	0.019	0.088	0.034	0.033	0.036	0.030	0.059	0.024	0.013	0.008	0.049	0.021	0.054	0.133	0.319	0.330	0.290	0.324	0.000	---
Mn	2.636	2.148	2.698	3.231	1.892	1.935	1.914	1.914	1.939	1.813	1.233	1.336	1.880	1.329	1.879	0.738	0.592	0.679	0.649	0.625	0.000	---
Fe2+	0.000	0.000	0.000	0.000	0.036	0.035	0.028	0.026	0.044	0.035	0.000	0.000	0.039	0.022	0.042	---	---	---	---	---	---	---
Zn	0.187	0.498	0.189	0.247	0.020	0.018	0.018	0.016	0.015	0.020	0.053	0.046	0.013	0.032	0.015	1.982	2.000	1.996	1.983	1.966	1.004	---
Ca	0.000	0.000	0.000	0.000	0.000	0.000	0.000	0.000	0.000	0.000	0.000	0.000	0.000	0.000	0.000	---	---	---	---	---	---	---
Li	0.738	0.456	0.709	0.712	0.622	0.630	0.618	0.632	0.622	0.665	0.651	0.632	0.696	0.785	0.706	0.000	0.000	0.000	0.000	0.000	0.000	---
Na	0.009	0.013	0.009	0.014	0.011	0.000	0.011	0.000	0.000	0.000	0.008	0.000	0.009	0.000	0.011	0.000	0.000	0.000	0.000	0.000	0.000	---
K	19.113	19.095	18.958	19.100	18.581	18.559	18.561	18.564	18.515	18.598	18.617	18.586	18.687	18.812	18.695	10.009	10.036	10.034	10.014	10.008	5.002	3.000
OH	4.000	3.645	4.000	3.707	3.778	3.661	3.772	4.000	3.715	3.749	4.000	4.000	4.000	3.745	4.000	1.000	1.000	1.000	1.000	1.000	---	0.821
F	0.000	0.355	0.000	0.293	0.222	0.339	0.228	0.000	0.285	0.251	0.000	0.000	0.000	0.255	0.000	0.000	0.000	0.000	0.000	0.000	---	0.179
O	27.000	27.000	27.000	27.000	27.000	27.000	27.000	27.000	27.000	27.000	27.000	27.000	27.000	27.000	27.000	15.000	15.000	15.000	15.000	15.000	8.000	3.000
Fe/Mn	127	184	141	37	57	60	55	65	33	76	99	162	39	63	36	6	2	2	2	2	---	---
F/OH	<0.10	0.22	<0.10	0.18	0.13	0.21	0.14	<0.10	0.17	0.15	<0.10	<0.10	<0.10	0.15	<0.10	0.00	0.00	0.00	0.00	0.00	---	0.49



TABLE 4. CHEMICAL COMPOSITION OF BERYL

	B1	B2	B3	B4	B5	B6	B7	B8	B9	B10	B11	B12	B13	B14	B15	B16	B17	B18	B19
SiO <sub>2</sub>	64.71	65.92	66.52	66.06	65.72	66.05	65.66	66.23	66.28	66.18	65.14	64.22	65.52	65.37	64.80	65.50	65.26	64.52	65.65
Al <sub>2</sub> O <sub>3</sub>	18.23	18.33	18.11	18.55	18.06	17.83	18.10	18.18	18.10	18.01	18.00	17.92	18.26	18.29	17.92	18.21	18.08	18.60	17.94
Sc <sub>2</sub> O <sub>3</sub>	0.02	0.00	0.00	0.00	0.00	0.00	0.00	0.00	0.00	0.00	0.00	0.00	0.00	0.00	0.00	0.00	0.00	0.00	0.00
V <sub>2</sub> O <sub>3</sub>	0.00	0.00	0.00	0.00	0.00	0.00	0.00	0.00	0.00	0.00	0.00	0.00	0.00	0.00	0.00	0.00	0.00	0.00	0.00
Cr <sub>2</sub> O <sub>3</sub>	0.00	0.00	0.00	0.00	0.00	0.00	0.00	0.00	0.00	0.00	0.00	0.00	0.00	0.00	0.00	0.00	0.00	0.00	0.00
Fe <sub>2</sub> O <sub>3</sub>	0.08	0.26	0.37	0.20	0.19	0.73	0.68	0.42	0.27	0.49	1.14	1.24	0.82	0.86	1.31	0.72	0.98	0.66	0.69
BeO *	13.57	13.75	13.85	13.88	13.73	13.74	13.71	13.78	13.78	13.74	13.65	13.49	13.72	13.70	13.61	13.70	13.66	13.57	13.67
MgO	0.04	0.19	0.32	0.08	0.07	0.13	0.14	0.11	0.00	0.00	0.16	0.16	0.18	0.16	0.20	0.17	0.17	0.11	0.16
MnO	0.00	0.00	0.00	0.00	0.00	0.00	0.00	0.00	0.00	0.00	0.00	0.00	0.00	0.00	0.00	0.00	0.00	0.00	0.00
CaO	0.00	0.00	0.00	0.00	0.00	0.00	0.00	0.00	0.00	0.00	0.00	0.00	0.00	0.00	0.00	0.00	0.00	0.00	0.00
Na <sub>2</sub> O	1.12	0.32	0.44	0.37	0.43	0.51	0.50	0.37	0.39	0.26	0.34	0.33	0.31	0.29	0.38	0.28	0.27	0.21	0.18
K <sub>2</sub> O	0.02	0.00	0.00	0.00	0.00	0.00	0.06	0.00	0.00	0.00	0.00	0.00	0.00	0.00	0.00	0.00	0.00	0.00	0.00
Cs <sub>2</sub> O	0.30	0.00	0.00	0.04	0.06	0.04	0.05	0.09	0.13	0.08	0.07	0.05	0.00	0.06	0.06	0.00	0.03	0.00	0.04
H <sub>2</sub> O *	1.30	0.37	0.51	0.43	0.50	0.60	0.58	0.43	0.45	0.30	0.40	0.39	0.36	0.34	0.45	0.33	0.32	0.25	0.21
	99.39	99.14	100.12	100.13	99.74	99.52	99.45	99.52	99.57	99.07	98.88	97.80	99.17	99.07	98.28	98.58	98.45	97.92	98.54

	B1	B2	B3	B4	B5	B6	B7	B8	B9	B10	B11	B12	B13	B14	B15	B16	B17	B18	B19
Si	11.911	11.976	11.994	11.984	11.953	11.957	11.958	12.007	12.014	12.030	11.918	11.886	11.926	11.916	11.894	11.943	11.930	11.872	11.993
Al	3.955	3.925	3.849	3.935	3.873	3.819	3.885	3.884	3.867	3.858	3.881	3.909	3.917	3.929	3.877	3.913	3.895	4.034	3.863
Sc	0.000	0.000	0.000	0.000	0.000	0.000	0.000	0.000	0.000	0.000	0.000	0.000	0.000	0.000	0.000	0.000	0.000	0.000	0.000
V	0.003	0.000	0.000	0.000	0.000	0.000	0.000	0.000	0.000	0.000	0.000	0.000	0.000	0.000	0.000	0.000	0.000	0.000	0.000
Cr	0.000	0.000	0.000	0.000	0.000	0.000	0.000	0.000	0.000	0.000	0.000	0.000	0.000	0.000	0.000	0.000	0.000	0.000	0.000
Fe <sub>3+</sub>	0.011	0.036	0.050	0.027	0.026	0.100	0.093	0.037	0.067	0.070	0.157	0.173	0.112	0.118	0.181	0.089	0.135	0.091	0.095
Be	6.000	6.000	6.000	6.000	6.000	6.000	6.000	6.000	6.000	6.000	6.000	6.000	6.000	6.000	6.000	6.000	6.000	6.000	6.000
Mg	0.011	0.051	0.086	0.021	0.019	0.035	0.065	0.030	0.000	0.000	0.044	0.044	0.049	0.043	0.055	0.046	0.046	0.030	0.044
Mn	0.000	0.000	0.000	0.000	0.000	0.000	0.000	0.000	0.000	0.000	0.000	0.000	0.000	0.000	0.000	0.000	0.000	0.000	0.000
Ca	0.000	0.000	0.000	0.000	0.000	0.000	0.000	0.000	0.000	0.000	0.000	0.000	0.000	0.000	0.000	0.000	0.000	0.000	0.000
Na	0.400	0.113	0.154	0.129	0.151	0.180	0.191	0.130	0.137	0.092	0.121	0.118	0.109	0.102	0.135	0.089	0.096	0.075	0.064
K	0.005	0.000	0.000	0.000	0.000	0.000	0.014	0.000	0.000	0.000	0.000	0.000	0.000	0.000	0.000	0.000	0.000	0.000	0.000
Cs	0.024	0.000	0.000	0.003	0.005	0.004	0.007	0.010	0.008	0.005	0.004	0.004	0.000	0.005	0.005	0.000	0.002	0.000	0.003
	22.320	22.100	22.133	22.100	22.126	22.148	22.177	22.101	22.091	22.055	22.125	22.134	22.114	22.114	22.147	22.100	22.104	22.103	22.062

	B1	B2	B3	B4	B5	B6	B7	B8	B9	B10	B11	B12	B13	B14	B15	B16	B17	B18	B19
H <sub>2</sub> O	0.800	0.226	0.308	0.258	0.302	0.360	0.352	0.382	0.274	0.184	0.242	0.236	0.218	0.204	0.270	0.198	0.192	0.150	0.128
O	36	36	36	36	36	36	36	36	36	36	36	36	36	36	36	36	36	36	36
Cs (ppm)	2900	<300	<300	370	600	360	430	890	1190	680	440	480	<300	560	560	<300	320	<300	380

Formula Contents per 36 (O)

\* H<sub>2</sub>O is a minimum estimate

TABLE 5. CHEMICAL COMPOSITION OF GARNET

	G1N	G1	G2	G3	G4	G5	G6	G7	G8	G9	G10	G11	G12	G13	G14	G15	G16	G17	G18
SiO2	36.27	36.58	36.17	36.09	36.02	36.16	35.99	36.54	35.41	36.54	36.38	36.09	36.11	35.65	35.10	35.80	36.61	36.42	36.38
P2O5	0.01	0.25	0.24	0.22	0.26	0.17	0.12	0.16	0.29	0.18	0.00	0.18	0.30	0.37	0.58	0.45	0.00	0.00	0.00
TiO2	0.13	0.00	0.00	0.00	0.00	0.00	0.00	0.00	0.08	0.09	0.00	0.13	0.00	0.00	0.14	0.11	0.00	0.00	0.00
Al2O3	20.51	20.52	20.69	20.79	20.54	20.66	20.69	20.58	20.30	20.68	20.73	20.35	19.99	20.16	19.88	20.25	20.71	20.70	20.76
Sc2O3	0.00	0.00	0.00	0.00	0.00	0.00	0.00	0.00	0.00	0.00	0.00	0.00	0.00	0.00	0.00	0.00	0.00	0.00	0.00
V2O3	0.00	0.00	0.00	0.00	0.00	0.00	0.00	0.00	0.00	0.00	0.00	0.00	0.00	0.00	0.00	0.00	0.00	0.00	0.00
MgO	0.34	0.30	0.21	0.25	0.25	0.36	0.51	0.54	0.93	1.35	0.94	0.34	0.42	0.77	0.77	0.99	1.20	1.52	1.46
MnO	20.07	17.79	17.61	17.61	17.61	18.35	17.71	17.37	23.67	13.65	7.98	17.13	25.91	26.17	26.00	23.77	7.76	5.97	6.05
FeO	15.45	24.86	25.24	25.02	24.83	24.03	24.97	24.86	18.14	27.12	33.10	24.92	16.93	15.94	16.22	17.72	32.15	33.82	34.00
CaO	6.04	0.41	0.41	0.39	0.41	0.51	0.34	0.50	0.19	0.49	0.67	0.46	0.18	0.24	0.18	0.23	1.55	1.36	1.43
Na2O	0.00	0.00	0.00	0.00	0.00	0.00	0.00	0.00	0.00	0.00	0.00	0.00	0.00	0.00	0.00	0.00	0.00	0.00	0.00
	98.82	100.71	100.57	100.37	99.92	100.24	100.33	100.55	99.01	100.10	99.80	99.60	99.84	99.30	98.87	99.32	99.98	99.79	100.08
<i>Formula Contents per 24 (O)</i>																			
Si	5.966	5.984	5.938	5.931	5.946	5.947	5.924	5.980	5.891	5.968	5.982	5.970	5.972	5.916	5.862	5.918	5.988	5.967	5.951
P	0.001	0.035	0.033	0.031	0.036	0.024	0.017	0.022	0.041	0.025	0.000	0.025	0.042	0.052	0.082	0.063	0.000	0.000	0.000
Ti	0.016	0.000	0.000	0.000	0.000	0.000	0.000	0.000	0.010	0.011	0.000	0.016	0.000	0.000	0.018	0.014	0.000	0.000	0.000
Al	3.976	3.956	4.003	4.027	3.996	4.005	4.013	3.970	3.980	3.981	4.017	3.968	3.896	3.943	3.913	3.945	3.992	3.997	4.002
Sc	0.000	0.000	0.000	0.000	0.000	0.000	0.000	0.000	0.000	0.000	0.000	0.000	0.000	0.000	0.000	0.000	0.000	0.000	0.000
V	0.000	0.000	0.000	0.000	0.000	0.000	0.000	0.000	0.000	0.000	0.000	0.000	0.000	0.000	0.000	0.000	0.000	0.000	0.000
Mg	0.083	0.073	0.051	0.061	0.062	0.088	0.125	0.132	0.231	0.329	0.230	0.084	0.104	0.190	0.192	0.244	0.293	0.371	0.356
Mn	2.796	2.465	2.449	2.451	2.462	2.556	2.469	2.408	3.336	1.888	1.111	2.400	3.630	3.678	3.678	3.328	1.075	0.828	0.838
Fe2+	2.125	3.401	3.465	3.439	3.428	3.305	3.437	3.403	2.524	3.705	4.551	3.448	2.342	2.212	2.265	2.450	4.397	4.634	4.651
Ca	1.064	0.072	0.072	0.069	0.073	0.090	0.060	0.088	0.033	0.086	0.118	0.082	0.032	0.043	0.032	0.041	0.272	0.239	0.251
Na	0.000	0.000	0.000	0.000	0.000	0.000	0.000	0.000	0.000	0.000	0.000	0.000	0.000	0.000	0.000	0.000	0.000	0.000	0.000
	16.028	15.986	16.011	16.009	16.002	16.015	16.045	16.002	16.046	15.993	16.010	15.992	16.017	16.035	16.041	16.002	16.016	16.035	16.048
O	24	24	24	24	24	24	24	24	24	24	24	24	24	24	24	24	24	24	24
% Alm	35	57	57	57	57	55	56	56	41	62	76	57	38	36	37	40	73	76	76
% Sp	46	41	41	41	41	42	41	40	54	31	18	40	59	60	60	55	18	14	14
% Gr	18	1	1	1	1	1	1	1	1	1	2	1	1	1	1	1	5	4	4
% Py	1	1	1	1	1	1	2	2	4	5	4	1	2	3	3	4	5	6	6
Fe/Mn	0.8	1.4	1.4	1.4	1.4	1.3	1.4	1.4	0.8	2.0	4.2	1.5	0.7	0.6	0.6	0.7	4.2	5.7	5.6
P (ppm)	<250	1100	1050	950	1150	750	500	700	1250	800	<250	1800	1300	1600	2500	2000	<250	<250	<250

TABLE 6. CHEMICAL COMPOSITION OF HFSE-SILICATE MINERALS

	TT1	TT2	TT3	TT4	TT5	TT6	TT7	TT8	TT9	A1	A2	A3	A4	A5	A6	A7	Z1	Z2	Z3	Z4		
SiO <sub>2</sub>	30.12	30.76	30.03	30.19	30.88	30.14	30.63	30.24	30.49	31.13	30.43	29.85	30.05	29.70	30.08	29.82	30.93	30.90	31.16	31.09		
TiO <sub>2</sub>	34.18	31.78	34.68	33.76	31.12	34.58	34.38	34.45	34.76	1.57	1.51	1.41	1.66	1.80	1.45	1.63	0.00	0.00	0.00	0.00		
SnO <sub>2</sub>	0.00	0.15	0.00	0.00	0.00	0.00	0.18	0.00	0.00													
ZrO <sub>2</sub>																						
HfO <sub>2</sub>																						
TiO <sub>2</sub>										1.18	1.20	2.22	1.40	0.96	1.34	1.25	1.56	1.74	1.78	2.02		
UO <sub>2</sub>										0.00	0.00	0.00	0.00	0.00	0.00	0.00	0.00	0.00	0.00	0.62		
Nb <sub>2</sub> O <sub>5</sub>	0.28	1.68	0.42	0.49	0.00	0.55	0.36	0.89	0.52													
Ta <sub>2</sub> O <sub>5</sub>	0.49	0.69	0.10	0.09	0.18	0.13	0.10	0.14	0.14													
Al <sub>2</sub> O <sub>3</sub>	2.35	3.70	2.16	2.56	5.08	2.43	2.67	2.35	2.28	13.27	13.28	12.67	12.18	12.17	12.78	12.34	0.00	0.00	0.00	0.62		
Fe <sub>2</sub> O <sub>3</sub> *										5.14	2.97	3.12	4.07	4.36	3.97	4.85	0.00	0.00	0.00	0.26		
Y <sub>2</sub> O <sub>3</sub>										0.00	0.00	0.00	0.00	0.00	0.00	0.00	0.94	0.86	0.67	0.26		
La <sub>2</sub> O <sub>3</sub>										10.24	10.50	10.45	9.51	9.96	9.23	9.64						
Ce <sub>2</sub> O <sub>3</sub>										10.73	10.36	10.66	11.37	11.07	11.68	10.75						
Pr <sub>2</sub> O <sub>3</sub>										0.61	0.63	0.51	0.80	0.79	0.65							
Nd <sub>2</sub> O <sub>3</sub>										1.13	1.30	1.26	1.54	1.54	1.60							
Yb <sub>2</sub> O <sub>3</sub>																						
MnO	0.08	0.19	0.14	0.10	0.20	0.12	0.18	0.16	0.09	0.43	0.27	0.26	0.63	0.59	0.61	0.50	0.00	0.40	0.00	0.00		
FeO	2.23	2.39	2.12	2.34	2.06	1.96	2.07	2.17	1.90	11.53	11.83	12.01	11.98	11.59	11.84	11.40	0.00	0.00	0.00	0.29		
CaO	27.58	27.97	27.36	27.11	29.40	27.74	28.28	27.77	27.49	11.42	10.94	10.56	10.41	10.47	10.37	10.71	0.00	0.00	0.00	0.08		
H <sub>2</sub> O*	0.77	0.56	0.81	0.72	0.44	0.55	0.71	0.57	0.69	1.55	1.50	1.47	1.49	1.38	1.49	1.48						
F	0.78	1.25	0.69	0.88	1.53	1.25	0.95	1.23	0.97	0.00	0.00	0.00	0.00	0.21	0.00	0.00						
O=F	-0.33	-0.53	-0.28	-0.37	-0.64	-0.53	-0.40	-0.52	-0.41	0.00	0.00	0.00	0.00	-0.09	0.00	0.00						
	98.53	100.59	98.78	98.57	100.43	98.26	100.30	99.77	99.29	99.93	96.72	96.45	97.09	96.50	97.26	96.43	99.20	100.67	99.62	99.35		
Si	3.970	3.988	3.954	3.984	3.984	3.946	3.966	3.946	3.982	3.013	3.046	3.036	3.033	3.012	3.023	3.013	1.012	0.997	0.997	0.981		
Ti	3.388	3.098	3.434	3.350	3.019	3.405	3.348	3.381	3.414	0.114	0.114	0.108	0.126	0.137	0.110	0.124	0.000	0.000	0.000	0.000		
Sn	0.000	0.009	0.000	0.000	0.000	0.000	0.009	0.000	0.000													
Zr																						
Hf																						
Th																						
U																						
Nb	0.017	0.098	0.025	0.029	0.000	0.033	0.021	0.053	0.031	0.026	0.027	0.051	0.032	0.022	0.031	0.029	0.011	0.007	0.003	0.011		
Ta	0.018	0.024	0.004	0.003	0.006	0.005	0.004	0.005	0.005								0.064	0.057	0.040	0.011		
Al	0.365	0.565	0.335	0.398	0.772	0.375	0.407	0.361	0.351	1.514	1.566	1.519	1.449	1.455	1.514	1.469	0.000	0.000	0.000	0.023		
Fe <sub>3</sub> <sup>+</sup>										0.374	0.224	0.239	0.309	0.333	0.300	0.368						
Y										0.366	0.388	0.392	0.354	0.373	0.342	0.359	0.016	0.015	0.016	0.018		
La										0.380	0.380	0.397	0.420	0.411	0.430	0.398	0.000	0.000	0.000	0.000		
Ce										0.022	0.023	0.019	0.029	0.029	0.030	0.024						
Pr										0.039	0.046	0.046	0.056	0.056	0.057	0.051						
Nd										0.035	0.023	0.022	0.054	0.051	0.052	0.043	0.000	0.004	0.000	0.000		
Yb	0.009	0.021	0.016	0.011	0.022	0.013	0.020	0.018	0.010	0.035	0.023	0.022	0.054	0.051	0.052	0.043	0.000	0.000	0.000	0.000		
Mn	0.246	0.259	0.233	0.258	0.222	0.215	0.224	0.237	0.208	0.934	0.960	1.022	1.012	0.983	0.995	0.963	0.000	0.000	0.000	0.008		
Fe <sub>2</sub> <sup>+</sup>	3.895	3.895	3.890	3.893	4.064	3.891	3.923	3.883	3.847	1.184	1.173	1.151	1.126	1.138	1.117	1.159	0.000	0.000	0.000	0.003		
Ca	11.908	11.947	11.888	11.901	12.097	11.898	11.932	11.898	11.868	8.000	8.000	8.000	8.000	8.000	8.000	8.000	2.005	2.005	2.001	2.013		
OH	0.675	0.488	0.713	0.633	0.376	0.482	0.611	0.492	0.599	1.000	1.000	1.000	1.000	0.933	1.000	1.000						
F	0.325	0.512	0.287	0.367	0.624	0.518	0.389	0.508	0.401	0.000	0.000	0.000	0.000	0.067	0.000	0.000						
O	19.000	19.000	19.000	19.000	19.000	19.000	19.000	19.000	19.000	12.000	12.000	12.000	12.000	12.000	12.000	12.000	4.000	4.000	4.000	4.000		
Nb/Ta	0.49	2.08	3.58	4.65	<0.50	3.61	3.07	5.43	3.17	>4.7	>4.7	>8.8	>5.5	>3.8	>5.5	>5.0	0.2	0.1	0.1	1.0		
Th/U																						
Zr/Hf																						

Formula Contents

Titanite formulae on 20 anions, allanite on 8 cations and 13 anions, Zircon on 4 (O).

TABLE 7. CHEMICAL COMPOSITION OF OXIDE MINERALS

	CT1	CT2	CT3	RT1	RT2	PR1	IL1	IL2	IL3	IL4	IL5	MT1	MT2	GN1	SC1
CaO	0.06	0.43	0.13	0.00	0.00	0.26	0.00	0.00	0.00	0.00	0.00	0.00	0.00	0.00	19.98
MgO	6.94	6.00	13.68	0.00	0.00	0.04	0.05	0.05	0.05	0.00	0.09	0.00	0.00	0.25	0.00
MnO	7.96	8.91	5.65	2.62	2.68	0.60	3.07	5.24	5.69	5.70	5.92	0.00	0.00	0.35	0.00
FeO	---	---	---	---	---	0.00	41.00	37.74	37.82	38.70	39.60	31.16	31.23	10.64	0.00
ZnO	---	---	---	---	---	0.58	---	---	---	---	---	---	---	28.89	---
Al <sub>2</sub> O <sub>3</sub>	---	---	---	---	---	0.00	---	---	---	---	---	---	---	57.24	---
Sc <sub>2</sub> O <sub>3</sub>	3.86	4.83	---	11.55	11.47	25.27	6.25	8.94	7.84	6.35	3.55	68.87	69.18	---	---
Fe <sub>2</sub> O <sub>3</sub> *	---	---	---	---	---	1.42	---	---	---	---	---	---	---	0.22	---
SiO <sub>2</sub>	2.28	4.55	1.50	51.55	52.06	66.21	48.34	47.63	48.24	49.14	50.88	0.10	0.06	---	0.00
TiO <sub>2</sub>	0.00	0.00	0.00	0.21	0.00	0.00	0.00	0.00	0.00	0.00	0.00	0.00	0.00	0.00	0.00
SnO <sub>2</sub>	38.44	55.09	64.52	20.54	21.17	0.93	0.68	0.28	0.27	0.26	0.00	0.00	0.00	0.00	0.00
Nb <sub>2</sub> O <sub>5</sub>	39.61	19.36	13.55	13.92	13.02	0.00	0.00	0.00	0.00	0.00	0.00	0.00	0.00	0.00	0.00
Ta <sub>2</sub> O <sub>5</sub>	---	---	---	---	---	---	---	---	---	---	---	---	---	---	2.35
MoO <sub>3</sub>	---	---	---	---	---	---	---	---	---	---	---	---	---	---	77.48
WO <sub>3</sub>	---	---	---	---	---	---	---	---	---	---	---	---	---	---	---
H <sub>2</sub> O	99.15	99.38	99.03	100.39	100.40	99.76	99.39	99.88	99.91	100.15	100.04	100.13	100.47	98.59	99.81

	Ca	Mg	Mn	Fe <sub>2</sub> <sup>+</sup>	Zn	Al	Sc	Fe <sub>3</sub> <sup>+</sup>	Si	Ti	Sn	Nb	Ta	Mo	W
Formula Contents	0.019	0.004	0.034	0.000	0.000	0.046	0.000	1.279	0.096	3.348	0.000	0.029	0.000	0.000	0.000
OH	---	---	---	---	---	---	---	---	---	---	---	---	---	---	---
O	24	24	1.5	24	24	24	24	24	24	24	24	24	24	24	24
Fe/Mn	1.2	1.5	0.4	>250	>250	>250	>250	>250	>250	>250	>250	>250	>250	>250	>250
Nb/Ta	0.8	2.4	4.1	1.3	1.4	1.4	1.4	1.4	1.4	1.4	1.4	1.4	1.4	1.4	1.4

Columbite-tantalite formulae on 12 cations and 24(O), rutile on 2 cations and 4(O), pseudobrookite on 10 anions, ilmenite on 2 cations and 3(O), magnetite on 3 cations and 4(O), garnite and scheelite on 4(O).

TABLE 8. CHEMICAL COMPOSITION OF PHOSPHATE MINERALS

	ALN	AP1	AP2	AP3	AP4	AP5	AP6	AP7	AP8	P1	P2	P3
Na <sub>2</sub> O	0.02	0.00	0.08	0.00	0.00	0.08	0.00	0.12	0.10	---	---	0.00
CaO	55.06	54.33	55.16	55.26	55.89	55.65	55.30	54.43	53.56	0.32	0.19	4.03
MgO	0.00	0.00	0.00	0.00	0.00	0.00	0.00	0.00	0.00	29.31	8.80	---
MnO	1.11	0.64	0.68	0.65	0.63	0.40	0.35	0.72	0.70	14.16	37.68	0.22
FeO	0.02	0.50	0.54	0.41	0.39	0.23	0.19	0.66	0.67	11.21	12.91	0.14
ZnO	---	---	---	---	---	---	---	---	---	0.81	1.19	---
SiO <sub>2</sub>	0.73	0.00	0.09	0.00	0.00	0.00	0.09	0.00	0.00	---	---	2.06
Y <sub>2</sub> O <sub>3</sub>	---	---	---	---	---	---	---	---	---	---	---	6.98
La <sub>2</sub> O <sub>3</sub>	---	---	---	---	---	---	---	---	---	---	---	18.84
Ce <sub>2</sub> O <sub>3</sub>	---	---	---	---	---	---	---	---	---	---	---	2.39
Pr <sub>2</sub> O <sub>3</sub>	---	---	---	---	---	---	---	---	---	---	---	7.92
Nd <sub>2</sub> O <sub>3</sub>	---	---	---	---	---	---	---	---	---	---	---	3.48
Sm <sub>2</sub> O <sub>3</sub>	---	---	---	---	---	---	---	---	---	---	---	2.57
Gd <sub>2</sub> O <sub>3</sub>	---	---	---	---	---	---	---	---	---	---	---	0.97
Dy <sub>2</sub> O <sub>3</sub>	---	---	---	---	---	---	---	---	---	---	---	12.53
ThO <sub>2</sub>	---	---	---	---	---	---	---	---	---	---	---	6.96
UO <sub>2</sub>	---	---	---	---	---	---	---	---	---	---	---	30.30
P <sub>2</sub> O <sub>5</sub>	41.76	43.14	42.75	42.81	43.03	42.53	43.31	42.39	42.98	38.87	34.78	---
H <sub>2</sub> O*	0.77	0.45	0.42	0.44	0.14	0.01	0.06	0.05	0.00	0.34	3.13	---
F	2.13	2.82	2.92	2.88	3.55	3.77	3.71	3.63	4.07	9.71	2.57	---
Cl	0.00	0.07	0.00	0.00	0.00	0.00	0.00	0.08	0.00	---	---	---
O=F,Cl	-0.90	-1.21	-1.23	-1.21	-1.49	-1.59	-1.56	-1.55	-1.71	-4.09	-1.08	---
	100.71	100.75	101.41	101.24	102.13	101.09	101.44	100.53	100.37	100.64	100.17	99.39

	ALN	AP1	AP2	AP3	AP4	AP5	AP6	AP7	AP8	P1	P2	P3
Na	0.006	0.000	0.026	0.000	0.000	0.026	0.000	0.039	0.032	---	---	0.000
Ca	9.912	9.671	9.802	9.822	9.861	9.921	9.782	9.764	9.562	0.010	0.007	0.674
Mg	0.000	0.000	0.000	0.000	0.000	0.000	0.000	0.000	0.000	1.326	0.452	---
Mn	0.158	0.090	0.096	0.091	0.088	0.056	0.049	0.102	0.098	0.364	1.100	0.029
Fe <sub>2</sub> +	0.002	0.069	0.075	0.057	0.054	0.032	0.026	0.092	0.093	0.285	0.372	0.018
Zn	---	---	---	---	---	---	---	---	---	0.018	0.030	---
Sr	0.072	0.000	0.009	0.000	0.000	0.000	0.009	0.000	0.000	---	---	0.171
Y	---	---	---	---	---	---	---	---	---	---	---	0.402
La	---	---	---	---	---	---	---	---	---	---	---	1.077
Ce	---	---	---	---	---	---	---	---	---	---	---	0.136
Pr	---	---	---	---	---	---	---	---	---	---	---	0.442
Nd	---	---	---	---	---	---	---	---	---	---	---	0.187
Sm	---	---	---	---	---	---	---	---	---	---	---	0.133
Gd	---	---	---	---	---	---	---	---	---	---	---	0.049
Dy	---	---	---	---	---	---	---	---	---	---	---	0.445
Th	---	---	---	---	---	---	---	---	---	---	---	0.242
U	5.940	6.068	6.002	6.012	5.999	5.991	6.054	6.009	6.063	0.999	1.015	4.004
P	16.092	15.898	16.009	15.982	16.002	16.026	15.920	16.006	15.849	3.002	2.976	8.009
OH	0.868	0.499	0.468	0.489	0.151	0.016	0.063	0.055	0.000	0.068	0.720	---
F	1.132	1.482	1.532	1.511	1.849	1.984	1.937	1.922	2.145	0.932	0.280	---
Cl	0.000	0.020	0.000	0.000	0.000	0.000	0.000	0.023	0.000	---	---	---
O	24.868	24.000	24.000	24.000	24.000	24.000	24.000	24.000	23.855	4.000	4.000	16.000
	26	26	26	26	26	26	26	26	26	5	5	16
Fe/Mn	0.0	0.8	0.8	0.6	0.6	0.6	0.5	0.9	1.0	0.8	0.3	0.6
Th/U	---	---	---	---	---	---	---	---	---	---	---	1.8
F/OH	3	7	7	7	27	>80	65	77	>80	30	1	---

Formula Contents

Apatite formulae on a basis of 26 anions, wagnerite and triplidite on 5 anions, monazite on 16 (O).

## APPENDIX 2: WHOLE-ROCK ANALYSES

### MAJOR ELEMENTS

	This Study	Gordey & Anderson (1993)	
		Average (13)	Standard Deviation
SiO <sub>2</sub>	65.29	65.1	2.0
TiO <sub>2</sub>	0.51, 0.47	0.60	0.07
Al <sub>2</sub> O <sub>3</sub>	14.12, 13.36	13.9	0.6
Fe <sub>2</sub> O <sub>3</sub>	1.59	1.1	0.3
FeO	2.55	3.1	0.4
MnO	0.07, 0.06	0.09	0.01
MgO	1.70, 1.48	2.16	0.68
CaO	3.73, 3.34	4.24	0.54
Na <sub>2</sub> O	2.49, 2.17	2.1	0.4
K <sub>2</sub> O	6.44, 5.55	5.76	1.18
P <sub>2</sub> O <sub>5</sub>	0.23, 0.22	0.25	0.04
H <sub>2</sub> O	0.52	0.7	0.2
CO <sub>2</sub>	< 0.2	0.1	0.2
Cl	0.0002	0.03	0.02
F	0.0015	0.12	0.02
S	0.04	0.02	0.03
Total	99.28	99.41	

In this study major elements were done using XRF. Where there are two numbers the second corresponds to a duplicate analysis by ICP. H<sub>2</sub>O by LOI, Cl by NAA.

TRACE ELEMENTS (ppm)

	This Study	Gordey & Anderson (1993)	
		Average (13)	Standard Deviation
Rb	352	325	66
Sr	392, 390 (ICP)	389	82
Ba	855, 780 (ICP)	848	341
U	26.6	18.0	7.0
Zr	180	217	22
Be	7.0 (ICP)	7.2	2.8
B	140	202	202
Li	84	51	11
As	4	3.6	1.9
Ag	< 0.2 (AAS)	0.2	0.1
Br	< 0.5	1	1
W	10 (ICP)	3	3
Sn	< 2	8	3
Mo	1 (ICP)	3	2
Co	9 (ICP)	13	5
Cr	205 (XRF), 181 (ICP)	40	31
Ni	44 (ICP)	20	7
V	73 (ICP)	89	28
Cu	26 (ICP)	16.3	7.9
Pb	40 (AAS)	40	7

TRACE ELEMENTS (ppm)

	This Study	Gordey & Anderson (1993)	
		Average (13)	Standard Deviation
Zn	52 (ICP)	56	5
La	62	110	24
Y	28	26.8	4.5
Yb	1.8		
Nb	20	24	6
Au	< 5 (ppb) (FA + AA)		
Bi	4 (ICP)		
Cd	< 0.5 (ICP)		
Cs	20.5 (NAA)		
Ga	14		
Rb/Sr	0.90, 0.90 (ICP)	0.85	0.19
K/Ba	62.6, 59.1 (ICP)	77.2	69.3
K/Rb	152, 131 (ICP)	151	24
Ba/Rb	3.33, 2.22 (ICP)	2.65	1.14